# Italian TRYs: New weather data impact on building energy simulations

Giorgio Lupato*, Marco Manzan

[a] *Department of Engineering and Architecture, University of Trieste, Trieste, Italy*

ARTICLE INFO

Accepted 1 December 2018

*Keywords:*
Weather files
Building energy simulations
Global warming

ABSTRACT

Dynamic thermal simulation is attracting the interest of designers thanks to the availability of numerical codes. However, one of the main problems facing the potential users is hourly-weather data availability. In Italy, the main source for the data is drawn upon the IGDG database. It is provided by the EnergyPlus weather site and the related measurements were collected between 1951 and 1970. A new set of files, gathered between 1989 and 2014, has recently become available. Nevertheless, it needs additional work to be directly implemented in energy simulation codes, which can lead users to download and apply the already available IGDG database files. In order to evaluate the ensuing effects, 52 Italian weather file locations were selected, and two simulations were carried out on seven multifamily-house models considering the difference between the results obtained using the old and new weather data. Since the locations of the two databases do not coincide, a matching method was implemented. This paper compares the simulation results arising from the choice of the weather file pertaining to the two databases. The weather files were selected within a 50 km range and 50 m elevation difference, to minimize misrepresentative results due to different climatic conditions. The models are typical of the most widespread building typology of the Italian building stock. For each model, two building fabric types were considered, the former was poorly insulated, the latter was well insulated thanks to an advanced refurbishment activity. Simulations were carried out with the EnergyPlus software.

## 1. Introduction

Computer-aided simulation is a powerful tool used by designers and researchers to study building energy aspects, including energy prediction and energy-cost analysis. Simulations are carried out with boundary conditions defined into a weather file that considerably affects energy outcomes. Despite weather data impact on building simulation results being widely analysed in literature, the topic is still meaningful especially because of climate change, which affects external building conditions.

Weather data are widespread and largely used in building simulations. In literature, the weather file impact was analysed in single simulations, multiple-years simulations and in building optimization. Typical weather data, for a one-year period, consists of hourly meteorological parameters obtained from long-term data. They can be generated using different calculation methodologies that aim to create some form of a most average year: it is a common approach [1] and it is generally preferred to AMY, that is recorded data spanning multiple years [2–4]. The climate parameters are connected with each other [5–7]: the methodologies to obtain reference years are expected to maintain cross-correlation between the climate data [8]. The typical meteorological year and the test reference year are the most popular methods in literature [2].

The test reference year is a weather file typology obtained from weather recordings statistically identified to compose a climatic representative year. The Finkelstein–Schafer statistic, described in EN ISO 15,927-4 technical standard [9], is an approach frequently found in literature to generate TRY [2,10]. Several methods were nonetheless developed both for TRY [2,11] and for TMY [12]. Sorrentino et al. [11] studied three statistical methods to calculate TRYs applied to a dataset collected in Palermo: he compared their impact on PV systems and building energy simulations. The results highlight a better performance for the Hall, Prairie, Anderson and Boes method. Pernigotto et al. [2] analysed six methodologies for the TRY definition and studied their applications to optimization, focusing on Pareto frontier results. The author used two datasets recorded in Trento and Monza: he showed that, by referring to the recommended insulation thickness, the impact of TRYs is low. However, the author also highlighted that the uncertainty related to energy and economic efficiency is relevant. Lupato et al. [13] achieved comparable results carrying out building optimizations with three TRYs obtained from different

* Corresponding author.
*E-mail address:* giorgio.lupato@phd.units.it (G. Lupato).

**Nomenclature**

| | |
|---|---|
| *HLS* | heat loss surface [$m^2$] |
| *M* | surface mass [$kg/m^2$] |
| $Q_{C,\ CTI}$ | cooling energy, CTI weather file [kWh] |
| $Q_{C,\ IGDG}$ | cooling energy, IGDG weather file [kWh] |
| $Q_{H,\ CTI}$ | heating energy, CTI weather file [kWh] |
| $Q_{H,\ IGDG}$ | heating energy, IGDG weather file [kWh] |
| $Q_{ins,C}$ | cooling energy, insulated building [kWh] |
| $Q_{ins,H}$ | heating energy, insulated building [kWh] |
| $Q_{unins,C}$ | cooling energy, uninsulated building [kWh] |
| $Q_{unins,H}$ | heating energy, uninsulated building [kWh] |
| *SV* | surface area to volume [$m^{-1}$] |
| *U* | thermal transmittance [$W{\cdot}m^{-2}{\cdot}K^{-1}$] |
| *Uw* | window thermal transmittance [$W{\cdot}m^{-2}{\cdot}K^{-1}$] |
| $\Delta Q_C$ | cooling energy difference [kWh] |
| $\Delta Q_H$ | heating energy difference [kWh] |
| $\Delta Q_{Sav,C}$ | cooling energy saving [kWh] |
| $\Delta Q_{Sav,H}$ | heating energy saving [kWh] |

*Acronyms*

| | |
|---|---|
| ACH | air changes per hour |
| AMY | actual meteorological year |
| $B_I$ | insulated building |
| $B_U$ | uninsulated building |
| CDD | cooling degree-day |
| CTI | Italian thermo-technical committee |
| DNI | direct normal solar radiation |
| E+ | EnergyPlus |
| EPPY | EnergyPlus Python library |
| HDD | heating degree-day |
| HVAC | heating ventilation and air conditioning |
| IDF | EnergyPlus model files |
| IGDG | Gianni De Giorgio weather file database |
| ISTAT | Italian national institute of statistics |
| NZEB | nearly zero energy building |
| PV | photovoltaic system |
| *SD* | standard deviation |
| SGHC | solar heat gain coefficient |
| TMY | typical meteorological year |
| TRY | test reference year |
| WWR | window wall ratio |

weather stations and recording-periods within the same location in Trieste.

Other authors focused on the impact of weather files considering different weather file types and real weather data. Crawley [14] presented results for an office building simulated with multiple-year weather data and different single-year weather dataset types for eight U.S. locations. He compared the influence of the various weather data sets on simulated annual energy use, costs and annual peak loads. Tianzhen et al. [15] analysed the weather impact on peak electric demand and energy use via building simulations using 30-year actual weather data for three types of office buildings at two design efficiency levels across all 17 climate zones. The simulated results from the AMY are compared to those from TMY3 to determine and analyse the differences. Also, Cui et al. [16] focused on actual weather data, comparing simulation results assessed with a 55-year dataset in 10 cities in China. The author underlined that weather varied significantly from year to year and typical year cannot reproduce the fluctuation: in particular, peak loads are more affected than energy consumption. Pernigotto et al. [17] studied the representativeness of EN ISO 15,927-4 method, applied to northern Italy climate. The author compared energy consumptions derived from the reference year and multi-year simulations and analysed energy variability.

TRY are generated using past weather data measurements. However, the efficiency of a refurbishing measure is assessed in the future, which is why numerous authors focused on applying future climate scenarios to building simulations, comparing energy demand and refurbishment effectiveness. Hosseini et al. [18] generated future weather condition files using a prediction model for roof design optimization. Huws and Jankovic [19] analysed the impact of retrofit measures on future carbon emissions using current and future climatic data. Ciulla et al. [20] adopted a similar approach to investigate the refurbishment effects on a social housing stock in Italy, highlighting the cost optimality of moderate measures. Eames et al. [21] investigated climate spatial distribution derived from UKCP09 weather generator, in the UK territory. The author studied both current and future climate change spatial variation scenarios, focusing on the differences of the UKCP09 adjacent areas. Rubio-Bellido et al. [22] investigated climate data for future scenarios and the effect on energy demand in office buildings in Chile. Unlike the previous cases, the author implemented the monthly model defined in EN ISO 13,790:2008 [23].

Considering the Italian climatic panorama, research was conducted on the effect of weather files and thus on building energy simulations. Chiesa and Grosso [24] performed a parametric study on the effect of different TMY. The author analysed three Italian cities with dynamic simulations and 21 Italian locations calculating CDD, HDD, annual global horizontal radiation and wind speed. As underlined by the author, further applications to a larger variety of climate zones and building types is expected to consolidate such outcomes.

Murano et al. [25] carried out a similar research, focusing on an NZEB single-family house and extended it to seven different locations which were representative of the Italian climate. The author highlighted the cooling and heating differences, calculating also the percentage differences. Pierangioli et al. [26] developed a refurbishment energy saving analysis based on six different buildings from the IEE TABULA [27] project method. Different building types were used: small multi-family houses, medium multi-family houses and apartment blocks. He carried out dynamic simulations using a representative weather file and two different future data sets obtained with morphing techniques related to the periods 2036–2065 and 2066–2095. He applied this methodology to two different locations in central Italy: Florence and San Vincenzo. The author focused on different design solutions selected with an energy-economic analysis.

The aim of this paper is to study the impact of the choice of weather files on building energy simulations, comparing the results obtained using two datasets recorded in different periods. The oldest, the IGDG dataset, is already available to the users through the EnergyPlus database. More recently, a new dataset has been provided by CTI, and has been generated using recent weather data measurements.

The results refer to the Italian multifamily-house stock and illustrate both energy consumption and energy savings, derived from refurbishment activities. The major objective of this work is to highlight the differences a practitioner can obtain in choosing an already available, but outdated dataset instead of a newer one. It is worth noting that the different results can be due to the period of data collection for weather file generation and possibly different locations, if the same site is not available in both datasets. To enhance the significance of the results the analysis covers the entire Italian territory analysing 52 locations. Furthermore, for each location the energy analysis is carried out on 7 buildings typologies considering also the effect of refurbishing activities. In author's knowledge, such analyses have never been realised considering the whole Italian territory and existing Italian building stock.

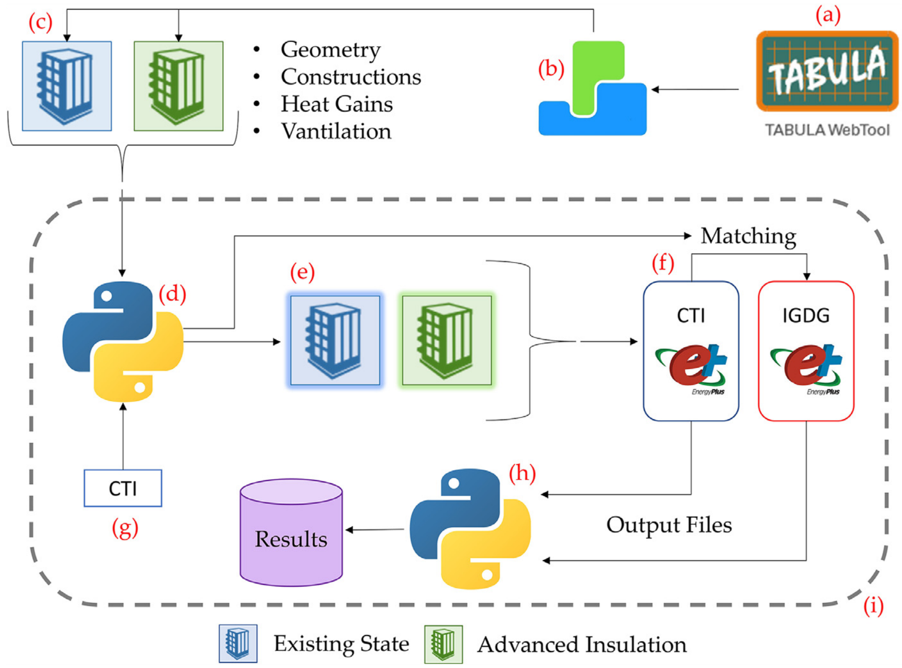


**Fig. 1.** Workflow scheme. (For interpretation of the references to colour in this figure, the reader is referred to the web version of this article.)

## 2. Methodology

As highlighted in the introduction, the locations in the territory and the building archetypes have a key role in the project. To operate with different weather data, locations and building fabrics, a procedure had to be implemented in order to run multiple simulations, to modify the building characteristics taking into account the location across the Italian territory and to collect the results. Furthermore, since the weather stations in the two datasets are not in the same position, a matching method is also needed.

The simulations workflow is summarized in Fig. 1: the red letters show the different steps of the implemented procedure. First, the models were obtained from TABULA data (a) and modelled with DesignBuilder [28] (b). The IDF file (EnergyPlus text model file) was exported (c) and edited with EPPY [29], a python scripting language precisely aimed at IDF editing (d) generating new IDF files referring to a specific simulation (e). The EPPY script in step (d) takes care of the matching between CTI and IGDG weather files (f) starting from the location of the CTI weather file (g).

The process required data related to the building location as an input: building location information and heating schedules, according to different climatic zones, were procedurally modified. Therefore, 52 models were obtained for every TABULA building, for both uninsulated and insulated buildings, for a total of 728 models (e).

Finally, within the same script, the simulations were carried out (f) and the related results were read from EnergyPlus output files and converted into dataframes for data analysis (h). The dotted box represents the iterative workflow (i), applied to all the not-rejected matchings obtained between the CTI and IGDG weather files. Section 3 describes the generation of building geometries and characteristics, Tables from 1 to 7 collect the main assumptions regarding building definitions. Section 4 presents the characteristics of the weather datasets used. The key problem in the comparison methodology between different datasets is the algorithm for selecting the pairs of location to be used in case weather stations do not coincide, to solve the problem the matching algorithm is presented in Section 5 with the selected pairs listed in Tables 8 and 9. The results are then analysed in Section 6.

**Table 1**
Buildings areas.

| Construction period | Area [m$^2$] | WWR [%] | Volume [m$^3$] | HLS [m$^2$] | SV [m$^{-1}$] |
|---|---|---|---|---|---|
| ...–1900 | 647 | 11.11 | 2684 | 1425 | 0.53 |
| 1921–1945 | 1165 | 11.99 | 4388 | 2243 | 051 |
| 1946–1960 | 961 | 20.84 | 3076 | 1551 | 0.50 |
| 1961–1975 | 934 | 9.33 | 3074 | 1667 | 0.54 |
| 1976–1990 | 1210 | 12.47 | 4136 | 1994 | 0.48 |
| 1991–2005 | 1120 | 14.56 | 3526 | 1763 | 0.50 |
| 2006–... | 915 | 13.92 | 2959 | 1357 | 0.46 |

## 3. Building model description

Tabula web tool [30] is a web service where European building stock data are provided, divided by age, size and country. External surfaces areas and the related thermal transmittances are given, for the original building, along with usual and advanced refurbishments. In this paper the insulated building corresponds to the advanced refurbishment solution of Tabula.

Tabula information was used to develop the geometry and the construction model. Since architectural drawings are not provided, the building geometry was obtained solving an equation system. The stairwell areas were not modelled. Tabula gives different building typologies: single family house, terraced house, multifamily house and apartment block. This research focuses on Italian multifamily houses, divided into eight different periods, from the construction age before 1900 until today. Building characteristics are summarized in Table 1.

### 3.1. Heat gains

Internal heat gains were modelled in accordance with EN ISO 13,790:2008 technical standard, where time-varying internal gains are described for living room, bedroom and kitchen room types. Since no zoning was defined in the models, a fixed space distribution was set to calculate heat gains, as shown in Table 2.

Electric heat gains can be summarized into a maximum design power of 4.6 W/m$^2$. Occupancy was set to a maximum of 0.04 people/m$^2$ with metabolic heating rate set to 110 W/person during day and 85 W/person at night.

**Table 2**
Space distribution within the thermal zones.

| Space type | Area % |
|---|---|
| Bedroom | 50 |
| Kitchen and living room | 35 |
| No gain areas | 15 |

According to the Italian regulations, the heating period during the year and the relative switch-on hours during the day were set depending on the climatic zone, which was calculated directly from CTI climatic files, considering the HDD. The adopted schedules are shown in Table 3.

Air temperature setpoint during the switch-on period was 20 °C, while for the remaining hours, a set-back air temperature of 18 °C was set. Cooling system availability was modelled as always-on during the whole year. The air temperature was set to 26 °C from 8 am to 10 pm: for the rest of the time, air temperature set-point was set to 28 °C. Heating and cooling schedules were modelled identically in both simulations, with CTI and IGDG weather files.

### *3.2. Heating and cooling systems types*

Heating and cooling systems types were modelled as ideal with 100% convective effects. It allowed the comparison of the energy consumption regardless the HVAC system typology. In order to model an ideal system, EnergyPlus [31] object ZoneHVAC: IdealLoadsAirSystem was used. It provides a model for an ideal HVAC system and it supplies cooling or heating air to a zone in sufficient quantity to meet the zone load. Cooling and heating thermal powers were modelled with unlimited capacity. Heating and cooling design supply conditions were modelled as shown in Table 4. Since cooling supply air conditions are far below zone internal air saturation conditions, latent gains were considered: the cooling system provides dehumidification. The ZoneHVAC: IdealLoadsAirSystem object is modelled as an ideal VAV terminal unit with variable supply air temperature and humidity. The supply air flow rate varies between zero and the maximum in order to satisfy the zone heating or cooling load.

### *3.3. Constructions*

Building constructions include both opaque and transparent components. Tabula web tool provides construction overall thermal transmittances which is why layers conductivity, thickness specific heat and density were obtained accordingly. As regards the transparent surfaces, Tabula thermal transmittance was used while SHGC was set between 0.9 and 0.7 in accordance with the construction year. SHGC of 0.398 was set for all refurbished buildings. Window wall ratios are illustrated in Table 1. Opaque and transparent constructions characteristics are summarized from Tables 5 to 7. The surface masses are reported in Table 6 for the uninsulated building only, since the values are not significantly affected by the application of an insulating material with low density. When two wall types were reported in Tabula web tool, the widest surface wall transmittance was selected: this case is highlighted with an asterisk (*) in Tables 5 and 6. No shadings were modelled during simulations to avoid human behaviour influences.

**Table 4**
Heating and cooling air inlet conditions.

| | Air temperature [°C] | Humidity ratio [$g_w/kg_{da}$] |
|---|---|---|
| Heating | 35 | 16 |
| Cooling | 12 | 8 |

### *3.4. Ventilation*

Outdoor air flow rate, intended as intentionally or inadvertently introduced into the building, is strictly dependent on the building construction performance and windows' openings. A total outdoor air change rate of 0.3 ACH was modelled as constant for both uninsulated and insulated models to have an analysis as objective as possible.

## **4. Weather files description**

The two weather datasets, IGDG and CTI, not only differ for the considered period but also for the generation methodology. The former database was obtained using measures collected between 1951 and 1970 and the calculation procedure is described by Mazzarella and Dati climatici [32], while the latter was obtained applying the procedures of EN ISO 15,927-4 technical standard based on Finkelstein–Schafer statistic and was generated using data collected between 1989 and 2014.

The IGDG weather files are available for download at EnergyPlus official web page [33], they are ready-to-use and do not need further data processing. However, even though CTI weather files are also freely available on the Italian thermo-technical committee website [34], they require additional processing to be used for dynamic building simulation. CTI files are provided with the following data, at an hour frequency:

- Dry bulb air temperature [°C]
- Relative humidity [%]
- Global solar radiation on horizontal plane [$W/m^2$]
- Direct solar radiation on horizontal plane [$W/m^2$]
- Diffuse solar radiation on horizontal plane [$W/m^2$]
- Vapor pressure [Pa]
- Wind speed [m/s]

In addition to the previous parameters, EnergyPlus requires dew point air temperature and direct normal solar radiation.

Since two psychrometric variables are given (dry bulb air temperature and relative humidity), the dew point air temperature was calculated.

Regarding solar data, EnergyPlus requires normal solar radiation in place of direct radiation on horizontal plane. However, the quantity is recorded using pyrheliometers. Such measuring instruments are rarely installed on weather stations owing to their high cost. In

**Table 3**
Climatic zone description with hour and date of heating system start-up and shutdown.

| Zone | From HDD | To HDD | Working-hours | Start date | End date | Start hour 1 | End hour 1 | Start hour 2 | End hour 2 |
|---|---|---|---|---|---|---|---|---|---|
| A | 0 | 600 | 6 | 01/12 | 15/03 | 8 | 11 | 19 | 22 |
| B | 601 | 900 | 8 | 01/12 | 31/03 | 8 | 12 | 18 | 22 |
| C | 901 | 1400 | 10 | 15/11 | 31/03 | 8 | 13 | 17 | 22 |
| D | 1401 | 2100 | 12 | 01/11 | 15/04 | 8 | 14 | 16 | 22 |
| E | 2101 | 3000 | 14 | 15/10 | 15/04 | 8 | 22 | – | – |
| F | 3001 | – | – | – | – | 0 | 24 | – | – |

**Table 5**
Opaque construction thermal transmittance for uninsulated and insulated models.

| OPAQUE U | ...–1900 | | 1921–1945 | | 1946–1960 | | 1961–1975 | | 1976–1990 | | 1991–2005 | | 2006–... | |
|---|---|---|---|---|---|---|---|---|---|---|---|---|---|---|
| | $B_U$ | $B_I$ | $B_U$ | $B_I$ | $B_U$ | $B_I$ | $B_U$ | $B_I$ | $B_U$ | $B_I$ | $B_U$ | $B_I$ | $B_U$ | $B_I$ |
| U Wall [W/m$^2$K] | 1.19 | 0.24 | 1.29* | 0.21 | 1.42* | 0.23 | 1.15* | 0.23 | 0.77* | 0.23 | 0.58* | 0.21 | 0.33* | 0.13 |
| U Roof [W/m$^2$K] | 1.28 | 0.21 | 1.48 | 0.21 | 1.10 | 0.21 | 1.10 | 0.21 | 0.75 | 0.21 | 0.57 | 0.21 | 0.28 | 0.13 |
| U Floor [W/m$^2$K] | 1.07 | 0.21 | 1.23 | 0.21 | 0.94 | 0.21 | 0.94 | 0.21 | 0.98 | 0.22 | 0.70* | 0.21 | 0.30 | 0.20 |

**Table 6**
Opaque construction surface mass for uninsulated and insulated models.

| OPAQUE M | ...–1900 | 1921–1945 | 1946–1960 | 1961–1975 | 1976–1990 | 1991–2005 | 2006–... |
|---|---|---|---|---|---|---|---|
| M Wall [kg/m$^2$] | 1267 | 155 | 737 | 194 | 176 | 203 | 160 |
| M Roof [kg/m$^2$] | 926 | 1210 | 406 | 406 | 276 | 277 | 278 |
| M Floor [kg/m$^2$] | 1096 | 1454 | 459 | 478 | 276 | 276 | 278 |

**Table 7**
Window characteristics for uninsulated and insulated models.

| WINDOW | ...–1900 | | 1921–1945 | | 1946–1960 | | 1961–1975 | | 1976–1990 | | 1991–2005 | | 2006–... | |
|---|---|---|---|---|---|---|---|---|---|---|---|---|---|---|
| | $B_U$ | $B_I$ | $B_U$ | $B_I$ | $B_U$ | $B_I$ | $B_U$ | $B_I$ | $B_U$ | $B_I$ | $B_U$ | $B_I$ | $B_U$ | $B_I$ |
| SHGC [–] | 0.9 | 0.398 | 0.9 | 0.398 | 0.75 | 0.398 | 0.7 | 0.398 | 0.7 | 0.398 | 0.9 | 0.398 | 0.9 | 0.398 |
| $U_w$ [W/m$^2$K] | 4.9 | 0.8 | 4.9 | 0.8 | 3.7 | 0.8 | 2.2 | 0.8 | 2.2 | 0.8 | 4.9 | 0.8 | 4.9 | 0.8 |


**Fig. 2.** Weather file locations, CTI in blue and IGDG in red. (For interpretation of the references to colour in this figure legend, the reader is referred to the web version of this article.)

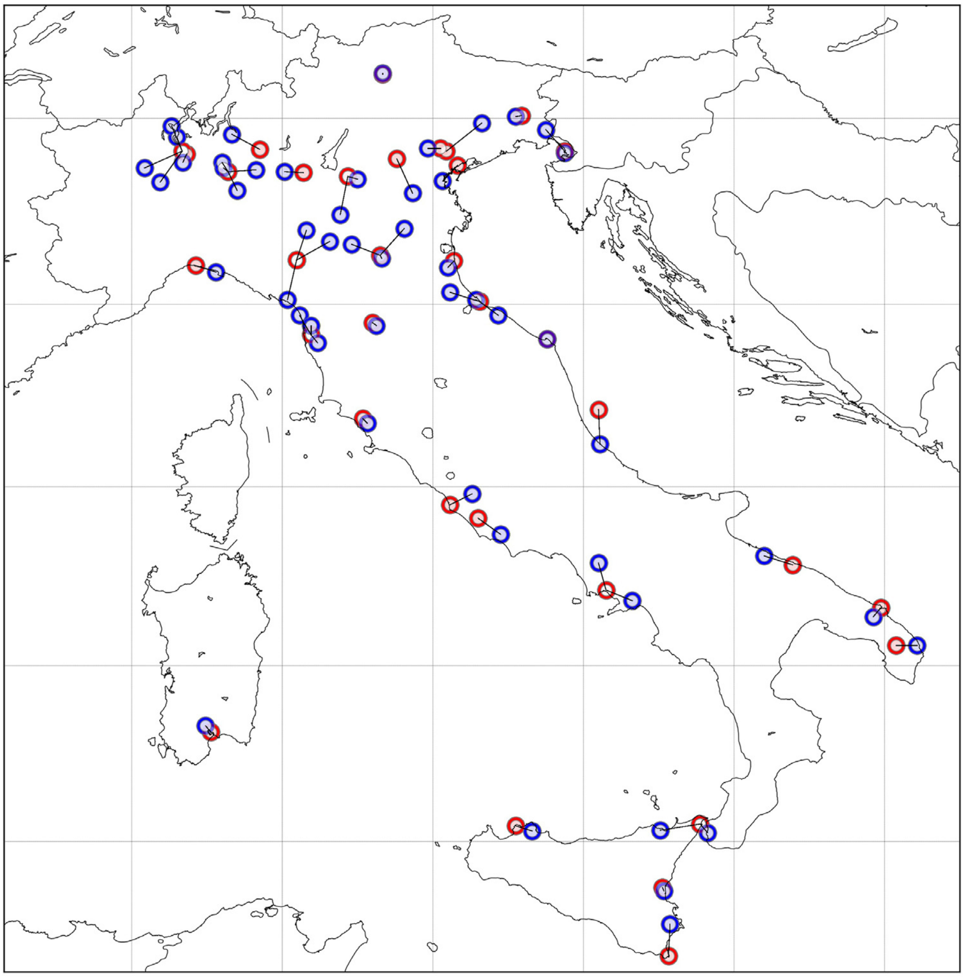

**Fig. 3.** Weather file matchings.

literature, many efforts were therefore made to develop solar radiation models that allow splitting global horizontal radiation into its components. Once the direct horizontal radiation is calculated, the standard approach to obtain DNI envisages dividing the direct horizontal radiation by the cosine of the zenith angle. Gueymard and Ruiz-Arias [35] evaluated the performance of 140 separation models and carried out a statistical study of models' results. Pernigotto et al. [36] investigated the impact of solar radiation models on building energy simulations in five European climates. Lupato et al. [37] carried out a similar research with a 10-year dataset recorded in Trieste, studying the energy variability of each year. In this paper, the Perez model highlighted the best overall performance and was thus applied to obtain DNI from the global solar radiation of CTI weather files.

In building energy simulations, ground temperature affects energy consumption, however the data are not provided by the weather files. A constant ground temperature of 18 °C was set to maintain the simulation as objective as possible.

## 5. Weather files matching

First of all, building simulations were carried out with CTI weather files. CTI files locations are widespread on the Italian territory and can represent most of the Italian climatic conditions, as illustrated by blue dots in Fig. 2.

In literature, little research was carried out to define a method for weather files' selection. Briggs et al. [38] developed a model to select the most representative weather files, considering HDD, CDD and the elevation difference between the building location and the weather station location. It was based on U.S. weather datasets and its application on Italian weather datasets led to poor outcomes: in some cases, northern locations were coupled to southern locations weather data. The poor results may be a consequence of the great diversity between the Italian and U.S. climatic conditions within the territory and country extensions. Moreover, the ASHRAE model refers to climatic parameters with a comparable record period which means that the assumption cannot be satisfied in the present case study.

As highlighted in EnergyPlus official documentation [39], it is recommended to select a weather file within a range of 50 km and 100 m elevation difference between the building location and the weather station. Therefore, a more restrictive limit of 50 km distance and 50 m elevation difference was set to select the related IGDG weather file. For every CTI location, distance and elevation difference related to IGDG dataset were calculated: all matchings that did not meet the requirements were rejected. This approach has been adopted possibly to replicate the choice a designer would operate in absence of local weather datasets.

Fulfilling the previously described conditions allows multiple IGDG stations to be selected for a single CTI location: in this specific case, the closest station was chosen, considering the distance parameter only.

The described method was applied to 108 CTI weather locations and resulted in a total of 52 valid matches which are shown in Fig. 3. Matching results are shown in Tables 8 and 9. In these tables, the CTI and the related IGDG station names are reported.

**Table 8**
Weather file matching results.

| *CTI Database* | | | | | | *IGDG Database* | | | | | | *Matching Values* | | | |
|---|---|---|---|---|---|---|---|---|---|---|---|---|---|---|---|
| *Station Name* | *Lat* [°] | *Lon* [°] | *Alt* [m] | *HDD* [-] | *CDD* [-] | *Selected Station Name* | *Lat* [°] | *Lon* [°] | *Alt* [m] | *HDD* [−] | *CDD* [−] | *Distance* [km] | *ΔHDD* [−] | *ΔCDD* [−] | *Δ Altitude* [m] |
| Abruzzo_Pescara | 42.47 | 14.22 | 5 | 2129 | 119 | ITA_Pescara.162300 | 42.85 | 14.2 | 16 | 2448 | 74 | 42 | −319 | 45 | −11 |
| Calabria_Reggio Calabria | 38.1 | 15.65 | 15 | 1268 | 194 | ITA_Messina.164200 | 38.2 | 15.55 | 59 | 1341 | 99 | 14 | −73 | 95 | −44 |
| Campania_Battipaglia | 40.73 | 14.65 | 55 | 1745 | 147 | ITA_Napoli-Capodichino.162890 | 40.85 | 14.3 | 72 | 2036 | 92 | 32 | −291 | 55 | −17 |
| Campania_Vitulazio | 41.15 | 14.2 | 65 | 1923 | 191 | ITA_Napoli-Capodichino.162890 | 40.85 | 14.3 | 72 | 2036 | 92 | 34 | −113 | 98 | −7 |
| Emilia Romagna_Bologna | 44.5 | 11.32 | 48 | 2696 | 87 | ITA_Bologna-Borgo.Panigale.161400 | 44.53 | 11.3 | 49 | 3000 | 126 | 4 | −305 | −38 | −1 |
| Emilia Romagna_Cesena | 44.13 | 12.23 | 42 | 2708 | 74 | ITA_Rimini.161490 | 44.03 | 12.62 | 13 | 2917 | 44 | 33 | −209 | 30 | 29 |
| Emilia Romagna_Ferrara | 44.82 | 11.62 | 6 | 2860 | 124 | ITA_Bologna-Borgo.Panigale.161400 | 44.53 | 11.3 | 49 | 3000 | 126 | 41 | −140 | −2 | −43 |
| Emilia Romagna_Modena | 44.65 | 10.92 | 37 | 2873 | 120 | ITA_Bologna-Borgo.Panigale.161400 | 44.53 | 11.3 | 49 | 3000 | 126 | 33 | −127 | −5 | −12 |
| Emilia Romagna_Parma | 44.8 | 10.32 | 57 | 2812 | 137 | ITA_Parma.161300 | 44.48 | 10.19 | 68 | 3194 | 68 | 37 | −383 | 69 | −11 |
| Emilia Romagna_Ravenna | 44.4 | 12.2 | 2 | 2772 | 69 | ITA_Marina.di.Ravenna. | 44.47 | 12.28 | 2 | 2762 | 45 | 10 | 10 | 24 | 0 |
| Emilia Romagna_Reggio Emilia | 44.68 | 10.63 | 56 | 2876 | 129 | ITA_Parma.161300 | 44.48 | 10.19 | 68 | 3194 | 68 | 41 | −319 | 61 | −12 |
| Emilia Romagna_Rimini | 44.05 | 12.57 | 7 | 2764 | 49 | ITA_Rimini.161490 | 44.03 | 12.62 | 13 | 2917 | 44 | 5 | −153 | 5 | −6 |
| FVG_Gradisca d'Isonzo | 45.88 | 13.5 | 30 | 2684 | 124 | ITA_Trieste.161100 | 45.65 | 13.75 | 20 | 2418 | 79 | 32 | 266 | 45 | 10 |
| FVG_Pordenone | 45.95 | 12.65 | 30 | 2804 | 96 | ITA_TrevisoS.Angelo.160990 | 45.65 | 12.18 | 18 | 2982 | 60 | 49 | −178 | 36 | 12 |
| FVG_Trieste - Molo Bandiera | 45.63 | 13.75 | 2 | 2034 | 71 | ITA_Trieste.161100 | 45.65 | 13.75 | 20 | 2418 | 79 | 2 | −384 | −8 | −18 |
| FVG_Udine | 46.02 | 13.1 | 80 | 2811 | 107 | ITA_Udine-Campoformido.160440 | 46.03 | 13.18 | 92 | 2977 | 73 | 6 | −167 | 35 | −12 |
| Lazio_Latina | 41.47 | 12.9 | 23 | 1760 | 178 | ITA_Pratica.di.Mare.162450 | 41.65 | 12.6 | 21 | 2222 | 41 | 32 | −463 | 137 | 2 |
| Lazio_Roma | 41.92 | 12.52 | 32 | 1859 | 193 | ITA_Roma-Fiumicino.162420 | 41.8 | 12.23 | 3 | 2113 | 70 | 27 | −255 | 124 | 29 |
| Liguria_Recco - Polanesi | 44.35 | 9.12 | 50 | 1706 | 75 | ITA_Genova-Sestri.161200 | 44.42 | 8.85 | 3 | 2055 | 37 | 23 | −350 | 38 | 47 |
| Lombardia_Bargnano | 45.43 | 10.03 | 93 | 3038 | 115 | ITA_Brescia-Ghedi.160880 | 45.42 | 10.28 | 102 | 3199 | 83 | 20 | −161 | 32 | −9 |
| Lombardia_Capralba | 45.45 | 9.65 | 96 | 3159 | 111 | ITA_Milano-Linate.160800 | 45.43 | 9.28 | 103 | 3097 | 77 | 29 | 62 | 34 | −7 |
| Lombardia_Cinisello Balsamo | 45.53 | 9.2 | 142 | 2815 | 165 | ITA_Milano-Linate.160800 | 45.43 | 9.28 | 103 | 3097 | 77 | 13 | −282 | 88 | 39 |
| Lombardia_Ispra | 45.8 | 8.6 | 193 | 2974 | 59 | ITA_Novara-Cameri.160640 | 45.65 | 8.67 | 178 | 3475 | 55 | 18 | −501 | 4 | 15 |
| Lombardia_Milano - via Juvara | 45.47 | 9.22 | 122 | 2562 | 119 | ITA_Milano-Linate.160800 | 45.43 | 9.28 | 103 | 3097 | 77 | 6 | −535 | 42 | 19 |
| Lombardia_Palidano di Gonzaga | 44.97 | 10.77 | 22 | 3019 | 166 | ITA_Verona-Villafranca.160900 | 45.38 | 10.87 | 68 | 3125 | 73 | 46 | −106 | 93 | −46 |
| Lombardia_S.Angelo Lodigiano | 45.23 | 9.4 | 60 | 2965 | 148 | ITA_Milano-Linate.160800 | 45.43 | 9.28 | 103 | 3097 | 77 | 24 | −131 | 71 | −43 |

**Table 9**
Weather file matching results.

| *CTI Database* | | | | | | *IGDG Database* | | | | | | *Matching Values* | | | |
|---|---|---|---|---|---|---|---|---|---|---|---|---|---|---|---|
| *Station Name* | *Lat* [°] | *Lon* [°] | *Alt* [m] | *HDD* [−] | *CDD* [−] | *Selected Station Name* | *Lat* [°] | *Lon* [°] | *Alt* [m] | *HDD* [−] | *CDD* [−] | *Distance* [km] | *ΔHDD* [−] | *ΔCDD* [−] | *Δ Altitude* [m] |
| Lombardia_Valmadrera | 45.83 | 9.33 | 237 | 2616 | 111 | ITA_Bergamo-Orio.al.Serio.160760 | 45.67 | 9.7 | 238 | 3208 | 48 | 34 | −592 | 64 | −1 |
| Marche_Ancona - Regione | 43.62 | 13.52 | 91 | 2155 | 96 | ITA_Ancona.161910 | 43.62 | 13.52 | 105 | 2302 | 38 | 0 | −146 | 58 | −14 |
| Marche_Villa Fastiggi | 43.88 | 12.87 | 20 | 2379 | 140 | ITA_Rimini.161490 | 44.03 | 12.62 | 13 | 2917 | 44 | 26 | −538 | 96 | 7 |
| Piemonte_Cameri | 45.53 | 8.68 | 173 | 3514 | 68 | ITA_Milano-Malpensa.160660 | 45.62 | 8.73 | 211 | 3487 | 50 | 11 | 27 | 17 | −38 |
| Piemonte_Massazza | 45.47 | 8.17 | 226 | 3220 | 63 | ITA_Novara-Cameri.160640 | 45.65 | 8.67 | 178 | 3475 | 55 | 44 | −255 | 8 | 48 |
| Piemonte_Pallanza | 45.92 | 8.53 | 202 | 2799 | 97 | ITA_Novara-Cameri.160640 | 45.65 | 8.67 | 178 | 3475 | 55 | 32 | −676 | 41 | 24 |
| Piemonte_Vercelli | 45.32 | 8.38 | 132 | 2984 | 124 | ITA_Novara-Cameri.160640 | 45.65 | 8.67 | 178 | 3475 | 55 | 43 | −491 | 68 | −46 |
| Puglia_Ver_3.1_Mesagne - Moccari | 40.55 | 17.85 | 53 | 1797 | 227 | ITA_Brindisi.163200 | 40.65 | 17.95 | 10 | 1707 | 90 | 14 | 89 | 137 | 43 |
| Puglia_Ver_3.1_Otranto | 40.23 | 18.43 | 24 | 1704 | 121 | ITA_Lecce.163320 | 40.23 | 18.15 | 48 | 1875 | 136 | 24 | −171 | −15 | −24 |
| Puglia_Ver_3.1_Trani | 41.23 | 16.4 | 63 | 1872 | 181 | ITA_Bari-Palese.Macchie.162700 | 41.13 | 16.78 | 49 | 1941 | 101 | 34 | −69 | 79 | 14 |
| Sardegna_Decimomannu | 39.32 | 8.98 | 20 | 1869 | 168 | ITA_Cagliari-Elmas.165600 | 39.25 | 9.05 | 18 | 1740 | 81 | 10 | 129 | 87 | 2 |
| Sicilia_Catania | 37.43 | 15.07 | 10 | 1467 | 216 | ITA_Catania-Fontanarossa.164600 | 37.47 | 15.05 | 17 | 1643 | 155 | 5 | −177 | 60 | −7 |
| Sicilia_Palermo | 38.12 | 13.32 | 50 | 1264 | 241 | ITA_Palermo-Punta.Raisi.164050 | 38.18 | 13.1 | 21 | 1164 | 77 | 20 | 100 | 164 | 29 |
| Sicilia_Patti | 38.13 | 15.02 | 70 | 1451 | 197 | ITA_Messina.164200 | 38.2 | 15.55 | 59 | 1341 | 99 | 47 | 110 | 97 | 11 |
| Sicilia_Siracusa | 37.05 | 15.15 | 90 | 1706 | 344 | ITA_Cozzo.Spadaro.164800 | 36.68 | 15.13 | 51 | 1286 | 119 | 41 | 420 | 226 | 39 |
| Toscana_Carrara | 44.05 | 10.07 | 90 | 2033 | 68 | ITA_Parma.161300 | 44.48 | 10.19 | 68 | 3194 | 68 | 49 | −1162 | 0 | 22 |
| Toscana_Collesalvetti | 43.58 | 10.47 | 15 | 2369 | 131 | ITA_Pisa-S.Gusto.161580 | 43.67 | 10.38 | 1 | 2424 | 70 | 12 | −54 | 61 | 14 |
| Toscana_Firenze | 43.77 | 11.25 | 70 | 2143 | 266 | ITA_Firenze-Peretola.161700 | 43.8 | 11.2 | 38 | 2535 | 126 | 5 | −393 | 140 | 32 |
| Toscana_Lido di Camaiore | 43.88 | 10.23 | 5 | 2284 | 116 | ITA_Pisa-S.Gusto.161580 | 43.67 | 10.38 | 1 | 2424 | 70 | 26 | −139 | 46 | 4 |
| Toscana_Rispescia | 42.7 | 11.13 | 40 | 2110 | 193 | ITA_Grosseto.162060 | 42.75 | 11.07 | 7 | 2337 | 123 | 7 | −227 | 70 | 33 |
| Toscana_San Giuliano Terme - Metato | 43.77 | 10.38 | 5 | 2272 | 87 | ITA_Pisa-S.Gusto.161580 | 43.67 | 10.38 | 1 | 2424 | 70 | 11 | −151 | 17 | 4 |
| Trentino Alto Adige_Bolzano | 46.48 | 11.33 | 265 | 2780 | 99 | ITA_Bolzano.160200 | 46.47 | 11.33 | 241 | 3663 | 65 | 1 | −882 | 34 | 24 |
| Veneto_Buttapietra | 45.35 | 11 | 39 | 2829 | 129 | ITA_Verona-Villafranca.160900 | 45.38 | 10.87 | 68 | 3125 | 73 | 11 | −296 | 56 | −29 |
| Veneto_Campagna Lupia - Valle Averto | 45.33 | 12.13 | 0 | 2751 | 113 | ITA_Venezia-Tessera.161050 | 45.5 | 12.33 | 10 | 2837 | 62 | 25 | −86 | 51 | −10 |
| Veneto_Castelfranco Veneto | 45.68 | 11.93 | 50 | 2922 | 140 | ITA_TrevisoIstrana.160980 | 45.68 | 12.1 | 45 | 3148 | 65 | 13 | −226 | 76 | 5 |
| Veneto_Monselice - Ca' Oddo | 45.2 | 11.73 | 6 | 2864 | 111 | ITA_Vicenza.160940 | 45.57 | 11.52 | 39 | 3078 | 86 | 44 | −215 | 24 | −33 |

Latitude, longitude, elevation, HDD and CDD are outlined for both weather files, as are distance, elevation, HDD and CDD difference between the two locations.

HDD and CDD were calculated with the methodology described in the UNI –EN-ISO 15,927-6:2008 technical standard [40]: heating and cooling baseline air temperature were set to 20 °C and 25 °C, respectively. During simulations, HDD and CDD calculations, no altitude correction was applied.

The latitude of Olbia reported in the IGDG file was found incorrect and the correct value 9.5° was inserted.

The inspection of Tables 8 and 9 shows, as a whole, a decrease in HDD between CTI and IGDG, which can be ascribed to an increase in external temperatures over the Italian territory, possibly due also to the climatic change. Though the TRY constitutes a form of average year [1], the energy consumption ensuing from the simulations is not always the average in the long term [15]. The TRYs are not the correct weather files to assess climate change. Indeed, in several cases, the test reference year leads to overestimation or underestimation of energy consumption or to a peak load demand [16]. However, the aim of choosing this methodology, is to compare the results that are achieved using TRY datasets calculated with different recording periods. Selecting the weather data location is always a critical aspect for performing an energy simulation, and this problem is even more critical if only a few dataset locations are available.

## 6. Discussion and results analysis

Since not all the results and graphs can be reported for each building type, only multifamily-house results from 1961 to 1975 are shown below. According to ISTAT data, this period is representative for the majority of the existing Italian buildings.

As previously explained, an ideal system was modelled. The system provides 100% convective heating and cooling: it allows to maintain the results as objective as possible, moving away from the system typology influence. Data analysis focuses on ideal energy consumption: no analysis of energy-cost or peak demand was carried out since the results are strictly related to HVAC systems. The main results are shown in Tables 11 and 12, related to uninsulated and insulated cases, respectively. In Tables 11 and 12, the first column reports the CTI station name while the remaining columns report heating and cooling energy for both weather files and their absolute difference.

The purpose of the following discussion is to analyse the weather file impact in terms of:

- Cooling and heating energy difference ($kWh/m^2$) between the two datasets.
- Cooling and heating energy difference ($kWh/m^2$) between the two datasets and the distribution across the Italianterritory.
- Cooling and heating energy ($kWh/m^2$) related to CTI: its variability within the datasets.
- Refurbishment energy saving difference ($kWh/m^2$) between the two datasets.

### *6.1. Cooling and heating difference*

Ideal heating and cooling energies were obtained using the two weather files for both uninsulated and insulated buildings thus allowing evaluating the energy difference, expressed in $kWh/m^2$. It

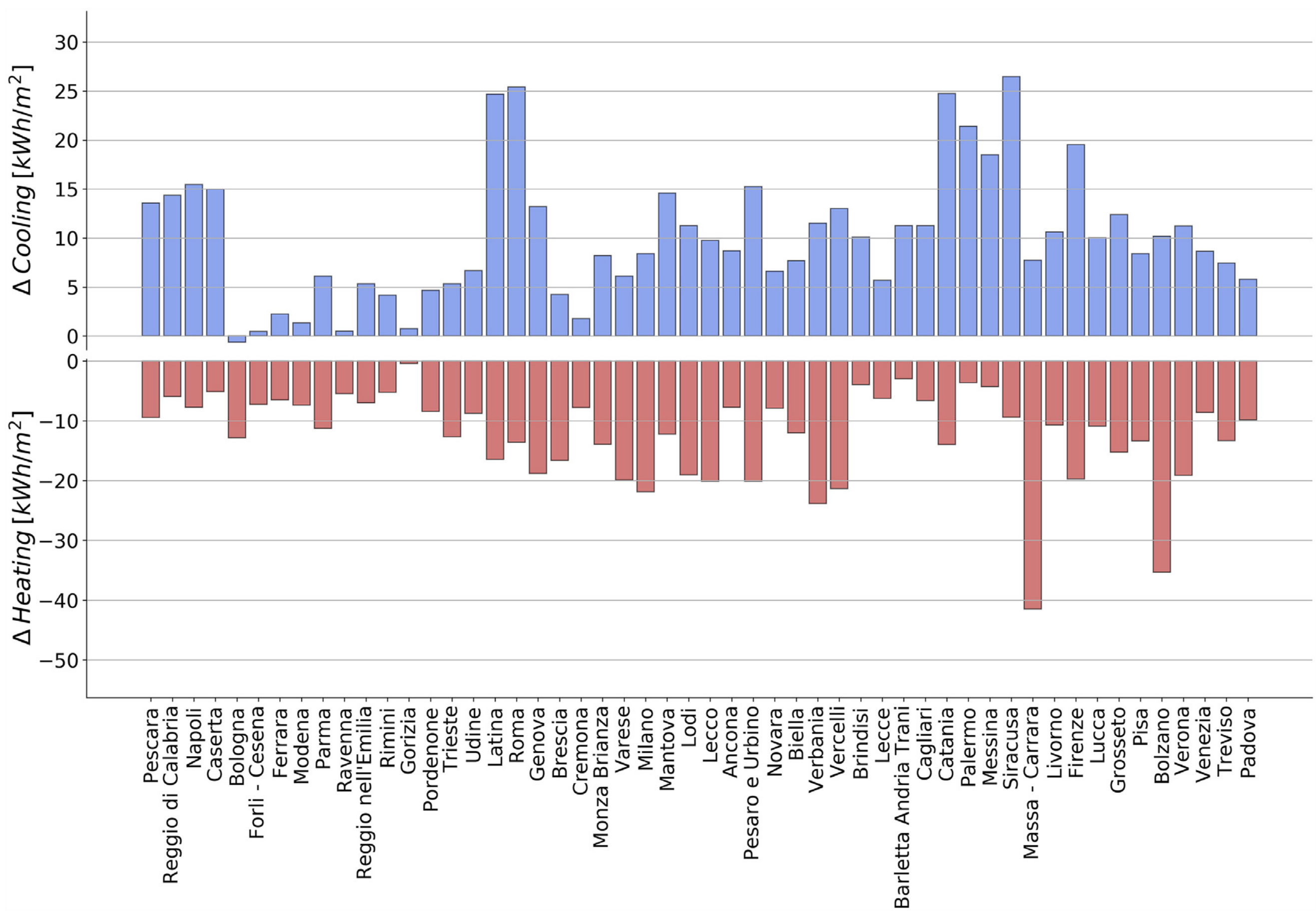


**Fig. 4.** Heating and cooling energy difference between CTI and IGDG weather files, uninsulated building. (For interpretation of the references to colour in this figure, the reader is referred to the web version of this article.)

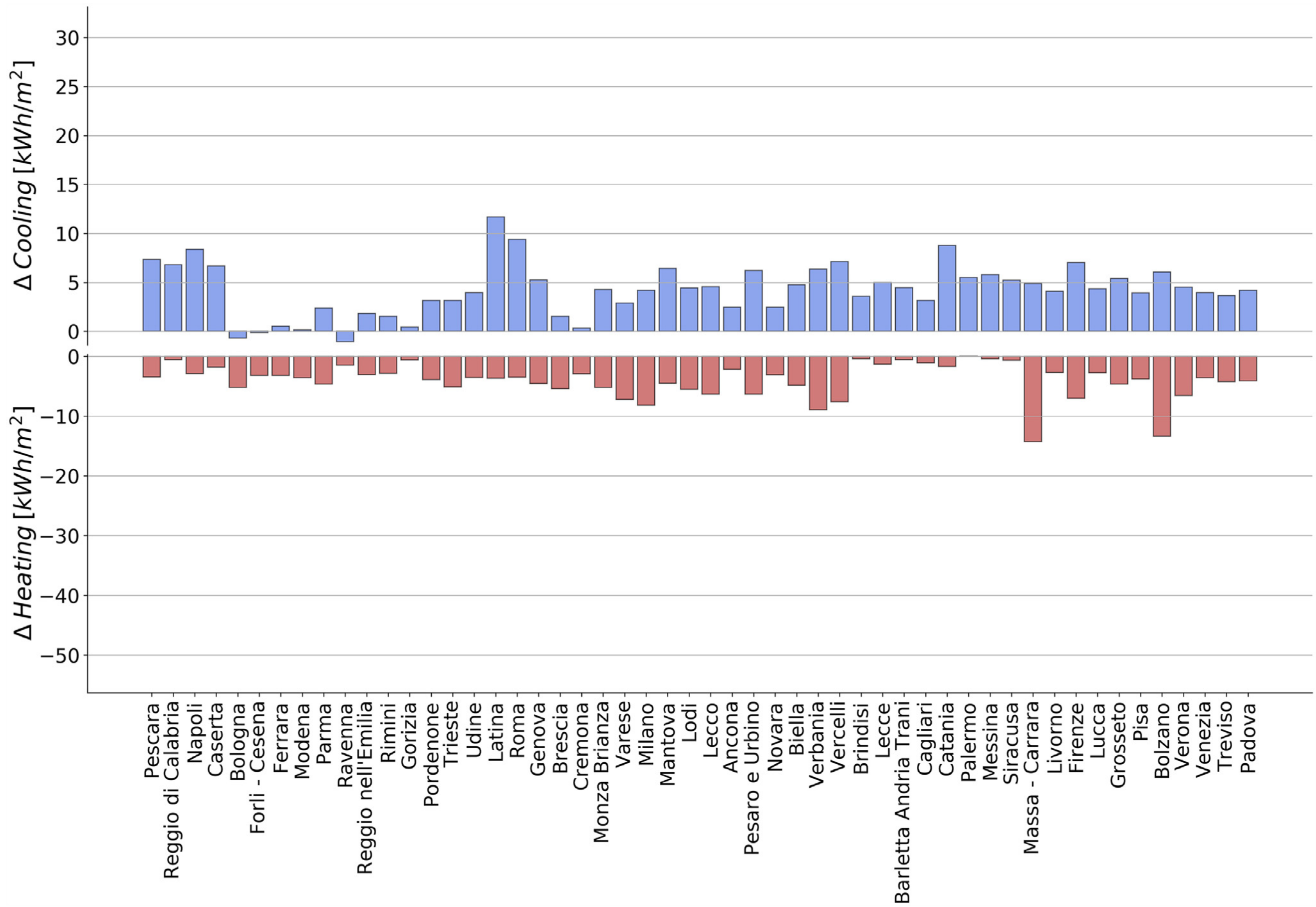


**Fig. 5.** Heating and cooling energy difference between CTI and IGDG weather files, insulated building. (For interpretation of the references to colour in this figure, the reader is referred to the web version of this article.)

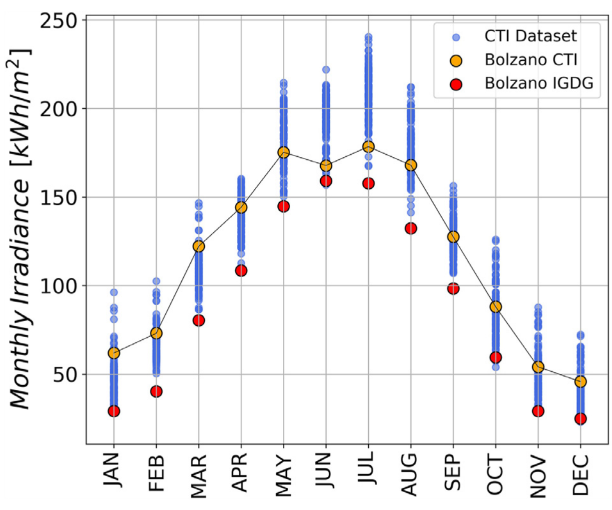


**Fig. 6.** Monthly global irradiance.

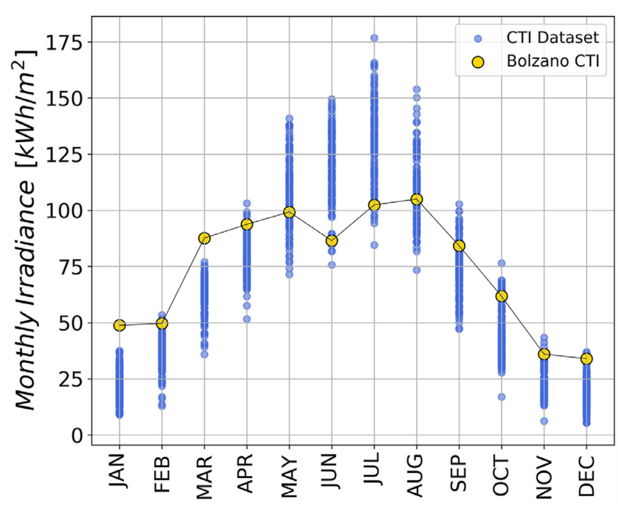


**Fig. 7.** Monthly direct irradiance.

was computed using the CTI and IGDG databases, respectively, calculated in accordance with Eqs. (1) and (2).

$$\Delta\ Q_C = Q_{C,\ CTI} - \ Q_{C,\ IGDG} \quad (1)$$

$$\Delta\ Q_H = Q_{H,\ CTI} - \ Q_{H,\ IGDG} \quad (2)$$

Results for uninsulated and insulated models are shown in Figs. 4 and 5 and the cooling and heating results are reported in blue and red, respectively. Regarding the uninsulated building, as can be noticed in Fig. 4, almost all the cooling energy differences are positive, while the heating differences are negative. Cooling energy consumption achieves a maximum increase of 26.5 $kWh/m^2$, mostly for southern locations. In accordance with cooling data, simulation results show heating energy consumption reduction, with a maximum decrease of almost 41.5 $kWh/m^2$.

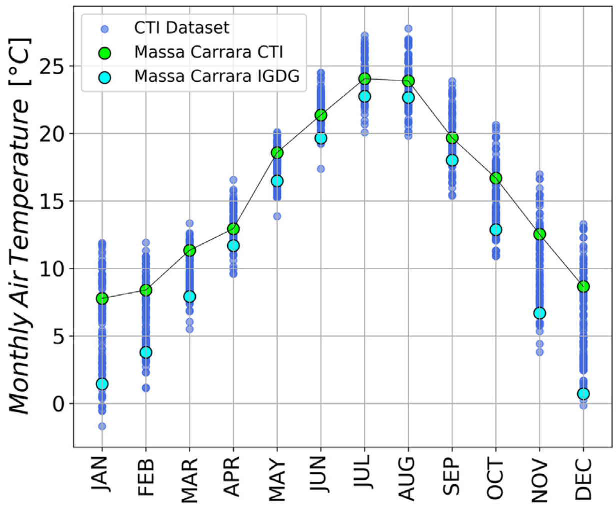


**Fig. 8.** Monthly dry-bulb air temperature.

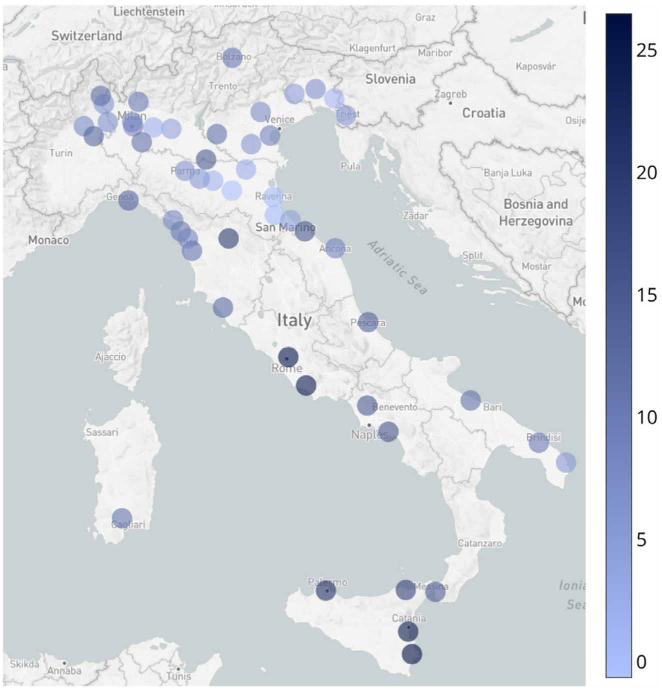


**Fig. 9.** Cooling energy difference distribution between CTI and IGDG weather files, uninsulated building [kWh/m$^2$].

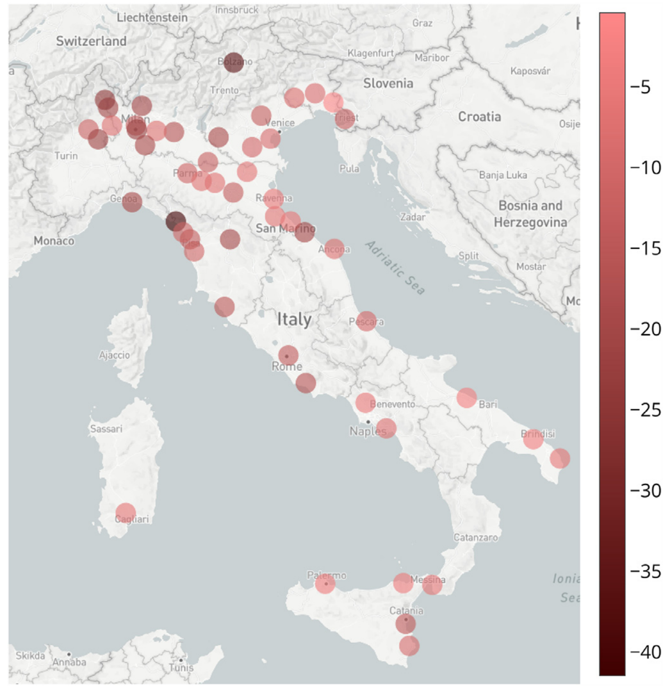


**Fig. 10.** Heating energy difference distribution between CTI and IGDG weather files, uninsulated building [kWh/m$^2$].

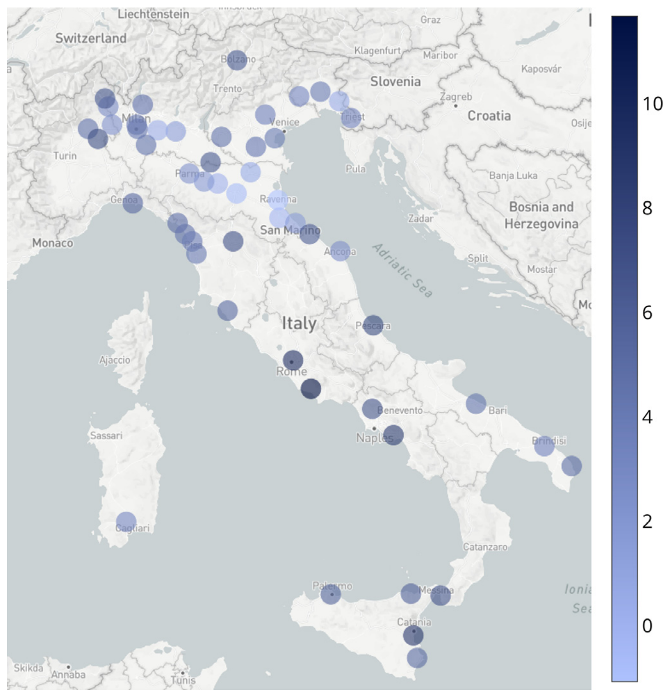


**Fig. 11.** Cooling energy difference distribution between CTI and IGDG weather files, insulated building [kWh/m$^2$].

Regarding the results for the insulated building, a similar trend can be noticed in Fig. 5, but it is characterized by lower energy reductions. The cooling and heating variations show a maximum of 11.7 kWh/m$^2$ and 14.3 kWh/m$^2$, respectively.

### *6.2. Maps*

Energy consumption differences between CTI and IGDG datasets are shown from Figs. 9 to 12. They were calculated in accordance with Eqs. (1) and (2). The dot colour intensity represents the energy difference. Different scales were used for uninsulated and insulated buildings. Representing such data on the map allows analysing their trends, also considering the territory distribution. As for cooling energy differences, they are more pronounced in southern areas, with a maximum along the Tyrrhenian coast and Sicily: the highest value is 26.5 kWh/m$^2$. Conversely, the differences are less significant in the Po Valley area. Regarding heating, northern Italian areas are more affected by the dataset selection; the inspection of Figs. 10 and 12 shows higher energy differences. However, Figs. 10 and 12 illustrate the presence of two outliers, characterized by a strong energy variation. They correspond to the locations of Massa-Carrara and Bolzano.

Monthly solar irradiation (kWh/m$^2$) and mean air temperature were studied to assess the results of Bolzano and Massa Carrara. Their CTI and IGDG values were compared to the entire CTI dataset,

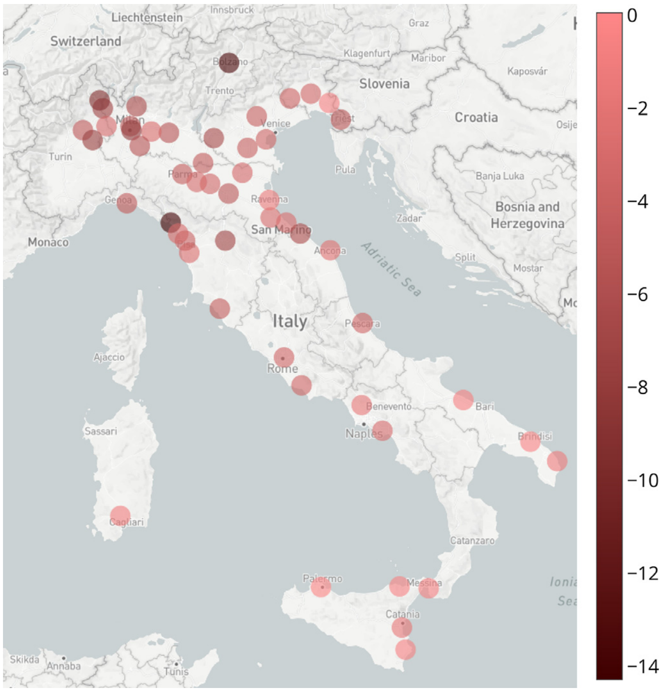


**Fig. 12.** Heating energy difference distribution between CTI and IGDG weather files, insulated building [kWh/m$^2$].

which, in this analysis includes all the data, not only those identified by the matching method.

Regarding Bolzano mean air temperature, no remarkable variations were appreciated: an overall increase was registered, comparable with other weather station data. Instead, as can be seen in Fig. 6, the global solar irradiation on horizontal plane, reported in the CTI dataset for Bolzano during winter, appears to be very high, both in terms of absolute and increasing value compared to the old IGDG data. Concerning the summer period, the opposite effect takes place: the irradiation is one of the lowest of the entire dataset. The direct component, presented in Fig. 7, leads to a quite astonishing result: irradiations are the highest within the dataset during winter and January and March irradiations stand above all the other data.

As for Massa Carrara, solar radiation increase is comparable to the dataset trend. Instead, a great increase of mean air temperature is shown in Fig. 8 during winter, while during summer the difference is moderate. The worst-case scenario is reported in December, when the mean air temperature moves from 0.7 °C to 8.7 °C. This variation explains the great heating energy reduction which could also be noticed analyzing the HDD variation. Their values are 2033 and 3194 for CTI and IGDG, respectively. Nevertheless, not all the air temperature increase is to be attributed to global warming: in this case the matching method linked a coastal city with an inland one. Furthermore, the Appennino Tosco-Emiliano National Park, located between the weather stations, contributes to the air temperature decrease. The territory topography thus affects the simulation outcomes highlighting the potential risk that can ensue by choosing the closest weather file from a less widespread and outdated dataset as the IGDG.

### 6.3. Cooling and heating distribution

Heating (red) and cooling (blue) energies related to CTI weather files are shown in Figs. 13 and 14: they include all year construction models' results. The same data are reported in Fig. 15 and Fig. 16 for the reference model. The plots are reported in pairs, for the uninsulated and the insulated models, respectively. The energy data are presented with the related IGDG consumptions on the $x$-axis: the continuous line represents the space where no energy variation occurred selecting a weather file or the other.

As shown in the figures Figs. 13 and 14, blue dots are placed above the line while the red lie below. It implies that, with more recent weather data, the cooling energy increases and the heating decreases.

Different axes' scales between uninsulated and insulated figures were set to maintain the figures' legibility. On the contrary, identical $x$-axis and $y$-axis scales were set within each figure. As highlighted in Fig. 15, cooling data are concentrated owing to the heating-based scale: cooling energy is lower than heating energy for uninsulated building. Nevertheless, the green dotted rectangle that contains cooling data shows a significantly greater height

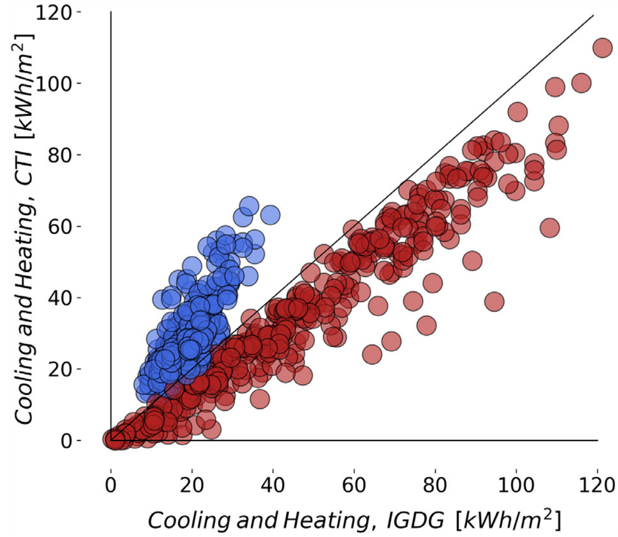


**Fig. 13.** CTI files heating and cooling energy: uninsulated building (all models). (For interpretation of the references to colour in this figure, the reader is referred to the web version of this article.)

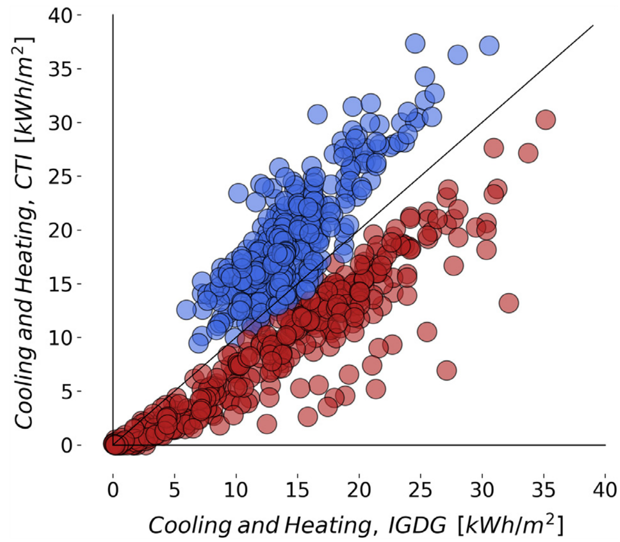


**Fig. 14.** CTI files heating and cooling energy: insulated building (all models). (For interpretation of the references to colour in this figure, the reader is referred to the web version of this article.)

**Table 10**
Cooling energy variability: standard deviation.

| | ...–1900 [kWh/m²] | 1921–1945 [kWh/m²] | 1946–1960 [kWh/m²] | 1961–1975 [kWh/m²] | 1976–1990 [kWh/m²] | 1991–2005 [kWh/m²] | 2006–... [kWh/m²] |
|---|---|---|---|---|---|---|---|
| $B_U$ IGDG | 4.47 | 4.39 | 5.09 | 4.39 | 3.29 | 3.7 | 4.02 |
| $B_U$ CTI | 9.84 | 9.42 | 10.38 | 8.93 | 6.23 | 7.03 | 6.81 |
| $B_I$ IGDG | 3.56 | 3.48 | 3.83 | 3.3 | 3.16 | 3.36 | 3.3 |
| $B_I$ CTI | 4.9 | 4.62 | 5.43 | 4.42 | 4.18 | 4.82 | 4.38 |

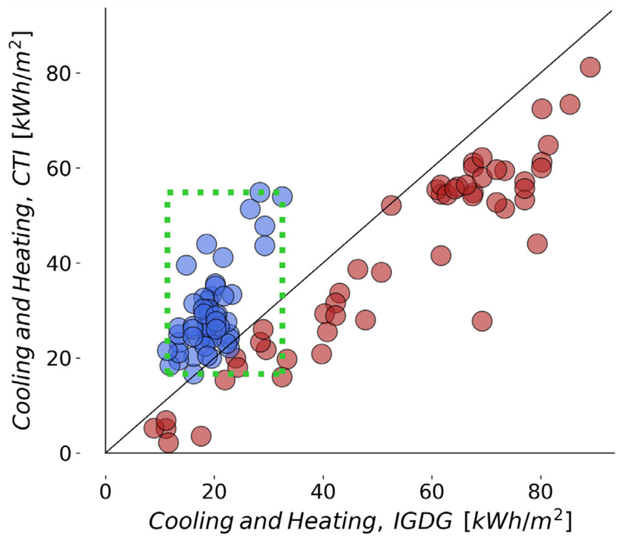


**Fig. 15.** CTI files heating and cooling energy: uninsulated building (reference model). (For interpretation of the references to colour in this figure, the reader is referred to the web version of this article.)

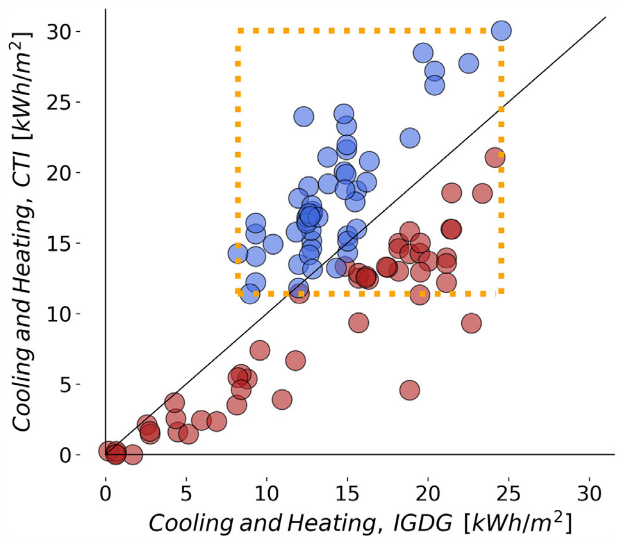


**Fig. 16.** CTI files heating and cooling energy: insulated building (reference model). (For interpretation of the references to colour in this figure, the reader is referred to the web version of this article.)

compared to its base: it indicates that the new weather files enhance energy consumption variability.

The opposite occurs when considering insulated building data in Fig. 16: cooling energy is predominant while heating and cooling variabilities are similar (height and base of the orange rectangle are comparable). The insulated model energy consumption is less dependent on climatic conditions and internal gains constitute a large part of the cooling load.

The energy consumption variabilities for insulated and uninsulated buildings (the green and orange boxes in Figs. 15 and 16) are analysed with standard deviation: the results are shown in Table 10 and were calculated using Eq. 3.

$$SD = \sqrt{\frac{\sum_{i=1}^{n} (x_i - \bar{x})^2}{n-1}} \quad (3)$$

### 6.4. Cooling and heating energy savings

Figs. 17 and 18 represent the energy savings in kWh/m$^2$ calculated as the difference between uninsulated and insulated energy consumption. Therefore, the renovation energy savings variation that could be achieved using a weather file or the other can be analysed. Energy savings are calculated in accordance with Eqs. (4) and (5).

$$\Delta Q_{Sav,C} = Q_{unins,C} - Q_{ins,C} \quad (4)$$

$$\Delta Q_{Sav,H} = Q_{unins,H} - Q_{ins,H} \quad (5)$$

With regard to cooling energy saving, while for the Po Valley area a slight difference is shown, higher differences are identified in southern locations. The ideal energy saving for Catania, Palermo, Messina and Syracuse ranges from 5.9 kWh/m$^2$ to 8.9 kWh/m$^2$ using the IGDG database and from 21.6 kWh/m$^2$ to 27.1 kWh/m$^2$ with the CTI files. Although for energy quantification an HVAC-system model is required, these variations are expected to affect the economic analyses significantly, which might include pay-back time and net present value. Various cities of central Italy highlight non-negligible differences: the values of Latina, Rome and Florence are 2.6 kWh/m$^2$, 3.8 kWh/m$^2$ and 6.7 kWh/m$^2$ for IGDG and increase to 15.6 kWh/m$^2$, 19.8 kWh/m$^2$ and 19.2 kWh/m$^2$ for CTI.

As for heating savings, the differences are less remarkable than those regarding the cooling scenario. Massa-Carrara and Bolzano present values of 50.4 kWh/m$^2$ and 56.7 kWh/m$^2$ for the IGDG file and of 23.2 kWh/m$^2$ and 34.7 kWh/m$^2$ for the CTI. However, these locations represent the outliers as reported in Section 6.2. Other significant results are recorded in Milan, Varese, Lecco, Pesaro and Urbino, Verbania, Vercelli, Florence and Verona. In general, refurbishment investments for heating energy savings would be less convenient when using the new CTI weather files instead of the older IGDG.

## 7. Conclusions

The impact of new weather data for energy building simulation, the CTI dataset, was analysed within the Italian panorama. Simulations were carried out with an outdated database, the already available IGDG, and the CTI dataset which requires some additional pre-process to be implemented. Unfortunately, the locations of the two databases do not coincide. Therefore, using the locations of the new datasets as a reference location, the comparison of the results

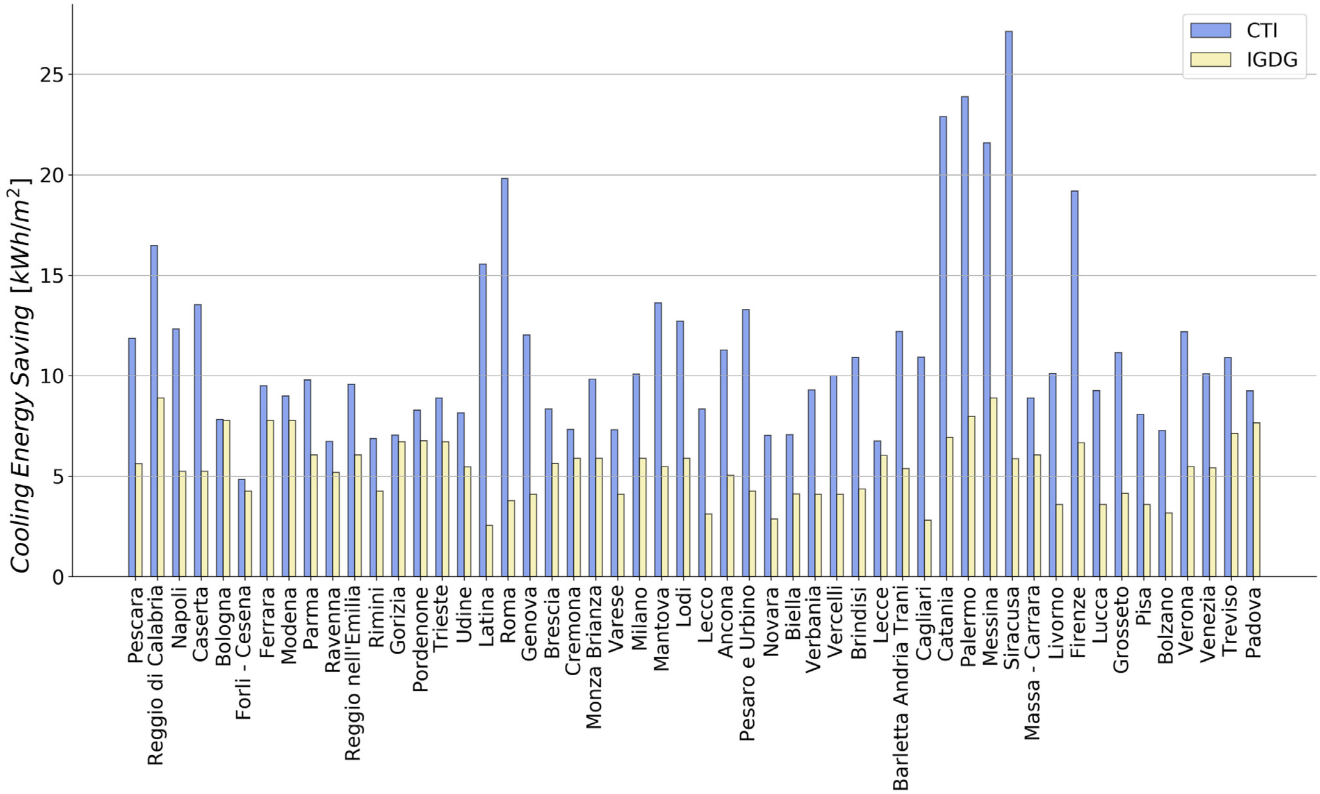


**Fig. 17.** Cooling energy savings for CTI and IGDG files.

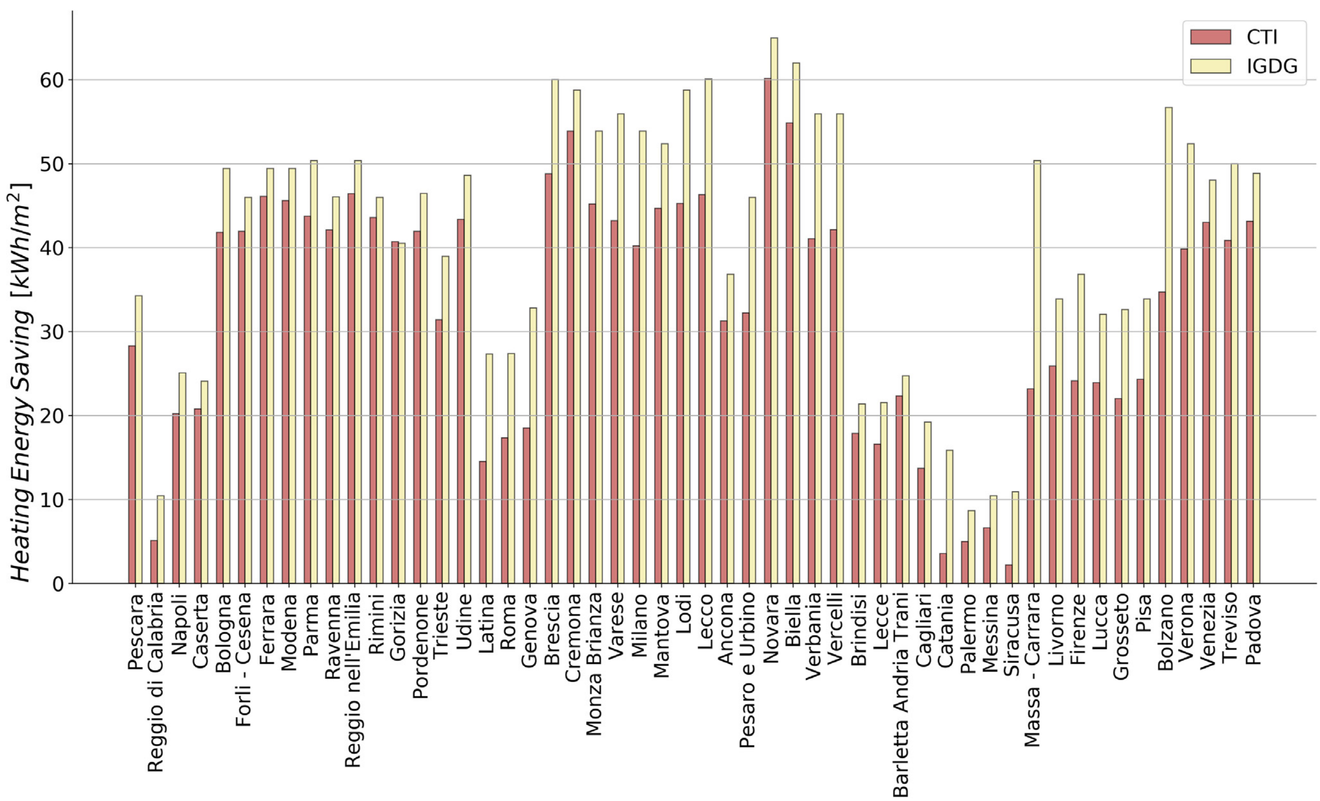


**Fig. 18.** Heating energy savings for CTI and IGDG files.

**Table 11**
Heating and cooling energy consumption for CTI and IGDG weather files, uninsulated building.

| CTI Station | Heating CTI [kWh] | Heating IGDG [kWh] | Cooling CTI [kWh] | Cooling IGDG [kWh] | Δ Heating [kWh] | Δ Cooling [kWh] |
|---|---|---|---|---|---|---|
| Abruzzo_Pescara_TRY.epw | 31,415 | 40,200 | 30,758 | 18,095 | −8785 | 12,664 |
| Calabria_Reggio Calabria_TRY.epw | 4840 | 10,377 | 40,758 | 27,333 | −5536 | 13,425 |
| Campania_Battipaglia_TRY.epw | 20,362 | 27,579 | 33,265 | 18,830 | −7217 | 14,435 |
| Campania_Vitulazio_TRY.epw | 21,787 | 26,568 | 32,810 | 18,830 | −4781 | 13,980 |
| Emilia Romagna_Bologna_TRY.epw | 51,139 | 63,099 | 20,669 | 21,266 | −11,960 | −598 |
| Emilia Romagna_Cesena_TRY.epw | 50,831 | 57,575 | 15,552 | 15,134 | −6743 | 418 |
| Emilia Romagna_Ferrara_TRY.epw | 57,033 | 63,099 | 23,359 | 21,266 | −6066 | 2092 |
| Emilia Romagna_Modena_TRY.epw | 56,206 | 63,099 | 22,523 | 21,266 | −6892 | 1256 |
| Emilia Romagna_Parma_TRY.epw | 54,120 | 64,615 | 23,290 | 17,581 | −10,495 | 5709 |
| Emilia Romagna_Ravenna_TRY.epw | 51,766 | 56,840 | 18,632 | 18,190 | −5075 | 442 |
| Emilia Romagna_Reggio Emilia_TRY.epw | 58,079 | 64,615 | 22,568 | 17,581 | −6537 | 4986 |
| Emilia Romagna_Rimini_TRY.epw | 52,691 | 57,575 | 19,014 | 15,134 | −4884 | 3879 |
| FVG_Gradisca d'Isonzo_TRY.epw | 48,658 | 49,048 | 21,506 | 20,805 | −391 | 701 |
| FVG_Pordenone_TRY.epw | 50,752 | 58,597 | 22,564 | 18,208 | −7845 | 4356 |
| FVG_Trieste - Molo Bandiera_TRY.epw | 35,530 | 47,348 | 25,776 | 20,805 | −11,818 | 4971 |
| FVG_Udine_TRY.epw | 52,290 | 60,452 | 22,338 | 16,123 | −8162 | 6215 |
| Lazio_Latina_TRY.epw | 14,930 | 30,293 | 36,898 | 13,859 | −15,363 | 23,039 |
| Lazio_Roma_TRY.epw | 18,458 | 31,118 | 41,046 | 17,333 | −12,660 | 23,713 |
| Liguria_Recco - Polanesi_TRY.epw | 19,486 | 37,058 | 29,950 | 17,627 | −17,572 | 12,323 |
| Lombardia_Bargnano_TRY.epw | 60,467 | 75,996 | 20,991 | 17,041 | −15,529 | 3949 |
| Lombardia_Capralba_TRY.epw | 67,629 | 74,894 | 19,116 | 17,465 | −7265 | 1652 |
| Lombardia_Cinisello Balsamo_TRY.epw | 55,497 | 68,487 | 25,135 | 17,456 | −12,990 | 7679 |
| Lombardia_Ispra_TRY.epw | 53,330 | 71,932 | 18,216 | 12,524 | −18,602 | 5692 |
| Lombardia_Milano - via Juvara_TRY.epw | 48,075 | 68,487 | 25,287 | 17,456 | −20,413 | 7831 |
| Lombardia_Palidano di Gonzaga_TRY.epw | 55,709 | 67,098 | 30,468 | 16,864 | −11,389 | 13,604 |
| Lombardia_S.Angelo Lodigiano_TRY.epw | 57,142 | 74,894 | 27,976 | 17,465 | −17,751 | 10,512 |
| Lombardia_Valmadrera_TRY.epw | 56,016 | 74,795 | 21,714 | 12,594 | −18,779 | 9120 |
| Marche_Ancona - Regione_TRY.epw | 36,097 | 43,298 | 27,257 | 19,151 | −7201 | 8106 |
| Marche_Villa Fastiggi_TRY.epw | 38,790 | 57,575 | 29,362 | 15,134 | −18,785 | 14,228 |
| Piemonte_Cameri_TRY.epw | 75,812 | 83,177 | 17,194 | 11,021 | −7365 | 6173 |
| Piemonte_Massazza_TRY.epw | 68,494 | 79,685 | 19,699 | 12,526 | −11,191 | 7173 |
| Piemonte_Pallanza_TRY.epw | 49,701 | 71,932 | 23,281 | 12,524 | −22,231 | 10,758 |
| Piemonte_Vercelli_TRY.epw | 51,988 | 71,932 | 24,663 | 12,524 | −19,944 | 12,140 |
| Puglia_Ver_3.1_Mesagne - Moccari_TRY.epw | 18,672 | 22,350 | 31,133 | 21,694 | −3679 | 9438 |
| Puglia_Ver_3.1_Otranto_TRY.epw | 16,843 | 22,660 | 24,859 | 19,548 | −5817 | 5312 |
| Puglia_Ver_3.1_Trani_TRY.epw | 24,299 | 27,066 | 30,806 | 20,290 | −2767 | 10,516 |
| Sardegna_Decimomannu_TRY.epw | 14,338 | 20,496 | 28,236 | 17,727 | −6158 | 10,508 |
| Sicilia_Catania_TRY.epw | 3346 | 16,378 | 47,949 | 24,850 | −13,033 | 23,099 |
| Sicilia_Palermo_TRY.epw | 4896 | 8285 | 50,343 | 30,355 | −3389 | 19,988 |
| Sicilia_Patti_TRY.epw | 6396 | 10,377 | 44,599 | 27,333 | −3980 | 17,266 |
| Sicilia_Siracusa_TRY.epw | 2056 | 10,810 | 51,218 | 26,492 | −8754 | 24,726 |
| Toscana_Carrara_TRY.epw | 25,909 | 64,615 | 24,790 | 17,581 | −38,706 | 7209 |
| Toscana_Collesalvetti_TRY.epw | 29,502 | 39,474 | 24,893 | 14,996 | −9973 | 9897 |
| Toscana_Firenze_TRY.epw | 26,174 | 44,595 | 38,423 | 20,173 | −18,421 | 18,250 |
| Toscana_Lido di Camaiore_TRY.epw | 27,413 | 37,574 | 24,346 | 14,996 | −10,161 | 9350 |
| Toscana_Rispescia_TRY.epw | 23,845 | 38,053 | 28,329 | 16,763 | −14,207 | 11,566 |
| Toscana_San Giuliano Terme - Metato_TRY.epw | 27,006 | 39,474 | 22,848 | 14,996 | −12,469 | 7852 |
| Trentino Alto Adige_Bolzano_TRY.epw | 41,114 | 74,099 | 20,104 | 10,605 | −32,986 | 9499 |
| Veneto_Buttapietra_TRY.epw | 49,256 | 67,098 | 27,345 | 16,864 | −17,842 | 10,482 |
| Veneto_Campagna Lupia - Valle Averto_TRY.epw | 51,861 | 59,899 | 26,970 | 18,906 | −8039 | 8064 |
| Veneto_Castelfranco Veneto_TRY.epw | 50,549 | 62,983 | 25,890 | 18,950 | −12,435 | 6940 |
| Veneto_Monselice - Ca' Oddo_TRY.epw | 52,693 | 61,873 | 24,384 | 18,977 | −9180 | 5406 |

was carried out every time that an IGDG file was found within a 50 km distance and 50 m height difference.

The simulations were applied to seven multifamily house models that are representative of the Italian building stock. For each model, two cases were studied: uninsulated and insulated constructions. For each location and building type, two numerical simulations were carried out using the two weather datasets giving rise to 728 simulations distributed across the Italian territory. As expected, the building performance is extremely affected by the choice of the weather dataset. The differences were highlighted using heating and cooling performance indicators: energy need difference, energy need and refurbishment energy savings.

As expected, heating energy decreases while cooling energy increases. However, energy need difference across the Italian territory showed a non-uniform distribution. The highest cooling energy differences occur in southern regions, especially along the Tyrrhenian coast. Regarding heating energy differences, northern locations generally result more affected by the weather file selection. No significant trend difference was identified for uninsulated and insulated buildings. The analysis allowed the identification of two outliers, Bolzano and Massa Carrara with a high decrease in heating energy. The Bolzano new weather file presents very high direct solar irradiance during the heating period which leads to a reduction of heating needs. For Massa Carrara, located on the shore, the matching algorithm selected an inland weather station, with lower temperatures not mitigated by the sea effect. The last result highlights the importance in choosing the weather files: the selection of the closest station, according to EnergyPlus documentation, can lead to significant errors in energy simulations. The problem draws attention to the risk that occurs selecting the

**Table 12**
Heating and cooling energy consumption for CTI and IGDG weather files, insulated building.

| CTI Station | Heating CTI [kWh] | Heating IGDG [kWh] | Cooling CTI [kWh] | Cooling IGDG [kWh] | Δ Heating [kWh] | Δ Cooling [kWh] |
|---|---|---|---|---|---|---|
| Abruzzo_Pescara_TRY.epw | 5007 | 8206 | 19,689 | 12,853 | −3200 | 6836 |
| Calabria_Reggio Calabria_TRY.epw | 71 | 616 | 25,384 | 19,040 | −545 | 6343 |
| Campania_Battipaglia_TRY.epw | 1505 | 4179 | 21,763 | 13,945 | −2674 | 7818 |
| Campania_Vitulazio_TRY.epw | 2389 | 4064 | 20,181 | 13,945 | −1676 | 6235 |
| Emilia Romagna_Bologna_TRY.epw | 12,125 | 16,973 | 13,366 | 14,013 | −4847 | −647 |
| Emilia Romagna_Cesena_TRY.epw | 11,688 | 14,652 | 11,035 | 11,163 | −2964 | −129 |
| Emilia Romagna_Ferrara_TRY.epw | 13,988 | 16,973 | 14,494 | 14,013 | −2985 | 481 |
| Emilia Romagna_Modena_TRY.epw | 13,635 | 16,973 | 14,137 | 14,013 | −3338 | 123 |
| Emilia Romagna_Parma_TRY.epw | 13,298 | 17,604 | 14,158 | 11,929 | −4306 | 2229 |
| Emilia Romagna_Ravenna_TRY.epw | 12,461 | 13,858 | 12,357 | 13,355 | −1396 | −998 |
| Emilia Romagna_Reggio Emilia_TRY.epw | 14,762 | 17,604 | 13,630 | 11,929 | −2842 | 1701 |
| Emilia Romagna_Rimini_TRY.epw | 12,015 | 14,652 | 12,595 | 11,163 | −2637 | 1432 |
| FVG_Gradisca d'Isonzo_TRY.epw | 10,659 | 11,215 | 14,929 | 14,536 | −556 | 393 |
| FVG_Pordenone_TRY.epw | 11,612 | 15,223 | 14,838 | 11,905 | −3611 | 2932 |
| FVG_Trieste - Molo Bandiera_TRY.epw | 6234 | 10,988 | 17,477 | 14,536 | −4754 | 2941 |
| FVG_Udine_TRY.epw | 11,808 | 15,090 | 14,729 | 11,031 | −3283 | 3698 |
| Lazio_Latina_TRY.epw | 1371 | 4801 | 22,377 | 11,478 | −3431 | 10,899 |
| Lazio_Roma_TRY.epw | 2280 | 5551 | 22,550 | 13,794 | −3271 | 8756 |
| Liguria_Recco - Polanesi_TRY.epw | 2208 | 6429 | 18,716 | 13,800 | −4221 | 4916 |
| Lombardia_Bargnano_TRY.epw | 14,931 | 19,990 | 13,214 | 11,781 | −5059 | 1433 |
| Lombardia_Capralba_TRY.epw | 17,332 | 20,040 | 12,279 | 11,973 | −2708 | 306 |
| Lombardia_Cinisello Balsamo_TRY.epw | 13,327 | 18,186 | 15,959 | 11,970 | −4859 | 3988 |
| Lombardia_Ispra_TRY.epw | 13,014 | 19,734 | 11,391 | 8690 | −6719 | 2701 |
| Lombardia_Milano - via Juvara_TRY.epw | 10,565 | 18,186 | 15,887 | 11,970 | −7621 | 3916 |
| Lombardia_Palidano di Gonzaga_TRY.epw | 14,009 | 18,215 | 17,750 | 11,753 | −4206 | 5996 |
| Lombardia_S.Angelo Lodigiano_TRY.epw | 14,912 | 20,040 | 16,104 | 11,973 | −5127 | 4131 |
| Lombardia_Valmadrera_TRY.epw | 12,806 | 18,700 | 13,938 | 9685 | −5895 | 4253 |
| Marche_Ancona - Regione_TRY.epw | 6913 | 8929 | 16,730 | 14,435 | −2016 | 2294 |
| Marche_Villa Fastiggi_TRY.epw | 8736 | 14,652 | 16,962 | 11,163 | −5916 | 5799 |
| Piemonte_Cameri_TRY.epw | 19,663 | 22,539 | 10,637 | 8352 | −2876 | 2285 |
| Piemonte_Massazza_TRY.epw | 17,294 | 21,817 | 13,115 | 8691 | −4523 | 4425 |
| Piemonte_Pallanza_TRY.epw | 11,388 | 19,734 | 14,609 | 8690 | −8346 | 5919 |
| Piemonte_Vercelli_TRY.epw | 12,652 | 19,734 | 15,332 | 8690 | −7082 | 6642 |
| Puglia_Ver_3.1_Mesagne - Moccari_TRY.epw | 1989 | 2403 | 20,951 | 17,620 | −413 | 3331 |
| Puglia_Ver_3.1_Otranto_TRY.epw | 1370 | 2571 | 18,570 | 13,924 | −1202 | 4646 |
| Puglia_Ver_3.1_Trani_TRY.epw | 3450 | 3987 | 19,413 | 15,262 | −538 | 4152 |
| Sardegna_Decimomannu_TRY.epw | 1545 | 2560 | 18,038 | 15,108 | −1015 | 2930 |
| Sicilia_Catania_TRY.epw | 1 | 1575 | 26,580 | 18,382 | −1574 | 8198 |
| Sicilia_Palermo_TRY.epw | 235 | 183 | 28,052 | 22,912 | 52 | 5140 |
| Sicilia_Patti_TRY.epw | 213 | 616 | 24,439 | 19,040 | −403 | 5399 |
| Sicilia_Siracusa_TRY.epw | 6 | 600 | 25,890 | 21,015 | −593 | 4875 |
| Toscana_Carrara_TRY.epw | 4269 | 17,604 | 16,490 | 11,929 | −13,334 | 4561 |
| Toscana_Collesalvetti_TRY.epw | 5321 | 7845 | 15,462 | 11,648 | −2524 | 3815 |
| Toscana_Firenze_TRY.epw | 3650 | 10,223 | 20,503 | 13,959 | −6574 | 6545 |
| Toscana_Lido di Camaiore_TRY.epw | 5109 | 7664 | 15,706 | 11,648 | −2555 | 4058 |
| Toscana_Rispescia_TRY.epw | 3298 | 7601 | 17,929 | 12,891 | −4304 | 5038 |
| Toscana_San Giuliano Terme - Metato_TRY.epw | 4306 | 7845 | 15,317 | 11,648 | −3539 | 3669 |
| Trentino Alto Adige_Bolzano_TRY.epw | 8710 | 21,176 | 13,314 | 7655 | −12,466 | 5659 |
| Veneto_Buttapietra_TRY.epw | 12,087 | 18,215 | 15,966 | 11,753 | −6128 | 4213 |
| Veneto_Campagna Lupia - Valle Averto_TRY.epw | 11,703 | 15,061 | 17,551 | 13,860 | −3358 | 3692 |
| Veneto_Castelfranco Veneto_TRY.epw | 12,395 | 16,333 | 15,718 | 12,305 | −3938 | 3414 |
| Veneto_Monselice - Ca' Oddo_TRY.epw | 12,426 | 16,258 | 15,758 | 11,837 | −3832 | 3921 |

weather file from the IGDG dataset, which is outdated and less widespread in the Italian territory.

Regarding cooling energy consumption, the results show that using the updated dataset for the uninsulated building entails an increase of energy consumption variability, which does not occur for insulated buildings. Instead, for heating energy, the variability remains unaffected.

Energy savings underline that, both for heating and cooling energy, the weather file selection could involve high differences. It emerged that the use of the outdated dataset leads to cooling savings underestimation and heating savings overestimation.

## Declaration of interest

None.


## Acknowledgement

This research did not receive any specific grant from funding agencies in the public, commercial, or nor-for-profit sectors.


## References


[1] K. Lee, H. Yoo, G.J. Levermore, Generation of typical weather data using the ISO Test Reference Year (TRY) method for major cities of South Korea, Build. Environ. 45 (4) (2010) 956–963 ISSN 0360-1323.

[2] G. Pernigotto, A. Prada, F. Cappelletti, A. Gasparella, Impact of Reference Years on the Outcome of Multi-Objective Optimization for Building Energy Refurbishment, Energies 10 (11) (2017) 1925 https://doi.org/10.3390/en10111925.

[3] T.L. Freeman, Evaluation of the 'Typical Meteorological Years' for Solar Heating and Cooling System Studies—Final, Report, Solar Energy Research Institute, Golden, CO, USA, 1979.

[4] R. Aguiar, S. Camelo, H Gonçalves, Assessing the value of typical meteorological years built from observed and from synthetic data for building thermal

simulation, in: Proceedings of the Sixth International IBPSA Conference, Kyoto, Japan, 1999.
[5] AHC Van Paassen, QX Luo, Weather data generator to study climate change on buildings, Build. Serv. Eng. Res. Technol. 23 (2002) 251–258.
[6] Aerographer's Mate, Module 05–Basic Meteorology, Integrated publishing, 2004 http://www.tpub.com/content/aerographer/14312/index.htm.
[7] L. Guan, J. Yang, J.M. Bell, Cross-correlations between weather variables in Australia, Build. Environ. 42 (2007) 1054–1070.
[8] H. Lund, The Design Reference Year Users Manual, DTU Thermal Insulation Laboratory, Copenhagen, Denmark, 1995.
[9] European Committee for Standardization (CEN), Standard EN ISO 15927-4, Hygrothermal Performance of Buildings–Calculation and Presentation of Climatic Data–Part 4: Hourly Data for Assessing the Annual Energy use for Heating and Cooling, 2005
[10] I.J. Hall, R.P. Richard, E.A. Herbert, C.B Eldon, Generation of Typical Meteorological Years for 26 SOLMET Stations, Sandia National Laboratories, Albuquerque, NM, USA, 1978 Technical Report SAND-78-1601.
[11] G. Sorrentino, G. Scaccianoce, M. Morale, V Franzitta, The importance of reliable climatic data in the energy evaluation, Energy 48 (2012) 74–79.
[12] K. Skeiker, Comparison of methodologies for TMY generation using 10 years data for Damascus, Syria, Energy Convers. Manag. 48 (2007) 2090–2102.
[13] G. Lupato, M. Manzan, A. Pezzi, The effect of climatic data on building performance optimization, in: Proceedings of the Building Simulation and Optimization 2018, Cambridge, UK, 2018 September 11-12, 2018, http://www.ibpsa.org/proceedings/BSO2018/6B-2.pdf.
[14] D.B. Crawley, Which weather data should you use for energy simulations of commercial buildings?, in: Transactions-American Society of Heating Refrigerating and Air Conditioning Engineers, 104, Ashrae American Society Heating Refrigerating, 1998, pp. 498–515.
[15] H. Tianzhen, C. Wen-Kuei, L. Hung-Wen, A sensitivity study of building performance using 30-year actual weather data, in: Proceedings of the BS2013: Thirteenth Conference of International Building Performance Simulation Association, Chambéry, France, 2013 August 26–28.
[16] Y. Cui, D. Yan, T. Hong, C. Xiao, X. Luo, Q Zhang, Comparison of typical year and multiyear building simulations using a 55-year actual weather data set from China, Appl. Energy 195 (2017) 890–904.
[17] G. Pernigotto, A. Prada, D. Cóstola, A. Gasparella, J.L.M Hensen, Multi-year and reference year weather data for building energy labelling in North Italy climates, Energy Build. 72 (2014) 62–72.
[18] M. Hosseini, F Tardy, B. Lee, Cooling and variety of roof designs; the effects of future weather data in a cold climate, J. Build. Eng. 17 (2018) 107–114 2352–7102.
[19] H. Huws, L. Jankovic, Optimisation of zero carbon retrofit in the context of current and future climate, in: Proceedings of the *Second IBPSA-England Conference BSO 2014*, London, 2014 23rd–24th June.
[20] G. Ciulla, A. Galatioto, R. Ricciu, Energy and economic analysis and feasibility of retrofit actions in Italian residential historical buildings, Energy Build. 128 (649–659) (2016) 0378–7788.
[21] M. Eames, T. Kershaw, D. Coley, The appropriate spatial resolution of future weather files for building simulation, J. Build. Perform. Simul. 5 (6) (2012) 347–358, doi:10.1080/19401493.2011.608133.
[22] C. Rubio-Bellido, A. Pérez-Fargallo, J.A. Pulido-Arcas, Optimization of annual energy demand in office buildings under the influence of climate change in Chile, Energy 114 (2016) 569–585 ISSN 0360-5442.
[23] European Committee for Standardization (CEN), Standard EN ISO 13790, Energy Performance of Buildings – Calculation of Energy Use for Space Heating and Cooling, 2008
[24] G. Chiesa, M. Grosso, The influence of different hourly typical meteorological years on dynamic simulation of buildings, Energy Proc. 78 (2015) 2560–2565 ISSN 1876-6102.
[25] G. Murano, V. Corrado, D. Dirutigliano, The new Italian climatic data and their effect in the calculation of the energy performance of buildings, Energy Proc. 101 (2016) 153–160 ISSN 1876-6102.
[26] L. Pierangioli, C. Carletti, G. Cellai, F. Sciurpi, Energy Refurbishment of social housing stock in Italy: analysis of some scenarios from the impact of climate change to occupant behaviour, in: *Proceedings of the Building Simulation Applications BSA* 2017, 8–10 February, Bolzano, Italy, 2017.
[27] Tabula project: http://episcope.eu/iee-project/tabula/ (11/10/2018).
[28] DesignBuilder, Version 5.0.3, (2017), DesignBuilder Software Limited.
[29] EPPY documentation https://pythonhosted.org/eppy/index.html (11/10/2018).
[30] Tabula web tool: http://webtool.building-typology.eu/ (01/08/2018).
[31] EnergyPlus, Version 8.6 (2016). U.S. Department of Energy.
[32] L. Mazzarella, G. Dati climatici, De Giorgio, in: Proceedings of the Giornata Di Studio Giovanni De Giorgio, Politecnico di Milano, Milano, 1997.
[33] Gianni De Giorgio TRY, EnergyPlus source (03/10/2018) https://energyplus.net/weather-region/europe_wmo_region_6/ITA%20%20.
[34] CTI TRY documentation (21/09/2018) https://try.cti2000.it/.
[35] C.A. Gueymard, J.A. Ruiz-Arias, Extensive worldwide validation and climate sensitivity analysis of direct irradiance predictions from 1-min global irradiance, Solar Energy 128 (2016) 1–30 ISSN 0038-092X.
[36] G. Pernigotto, A. Prada, P. Baggio, A. Gasparella, A. Mahdavi, Solar irradiance modelling and uncertainty on building hourly profiles of heating and cooling energy needs, in: Proceedings of the International High Performance Buildings Conference, 2016.
[37] G. Lupato, M. Manzan, S. Cirilli, Comparison of direct radiation split algorithms for energy simulation of buildings, in: *Proceedings of the Building Simulation Applications BSA 2017, 8–10 February*, Bolzano, Italy, 2018.
[38] R.S. Briggs, Z.T. Taylor, G.L. Robert, Climate classification for building energy codes and standards: Part 2-zone definitions, maps and comparisons, Energy Proc. 78 (2560–2565) (2003) 1876–6102.
[39] EnergyPlus official documentation: https://energyplus.net/weather/simulation (01/08/2018)
[40] European Committee for Standardization (CEN), Standard EN-ISO 15927-6, Hygrothermal Performance of Buildings – Calculation and Presentation of Climatic Data Accumulated Temperature Differences ( Degree-Day), 2008